

# Retinotectal Mapping: New Insights from Molecular Genetics

Greg Lemke<sup>1</sup> and Michaël Reber<sup>2</sup>

<sup>1</sup>Molecular Neurobiology Laboratory, The Salk Institute, La Jolla, California 92037; email: lemke@salk.edu

<sup>2</sup>INSERM U.575-Centre de Neurochimie, 67084 Strasbourg, France; email: michael.reber@inserm.u-strasbg.fr

Annu. Rev. Cell Dev. Biol.  
2005. 21:551–80

First published online as a  
Review in Advance on  
June 29, 2005

The *Annual Review of  
Cell and Developmental  
Biology* is online at  
<http://cellbio.annualreviews.org>

doi: 10.1146/  
annurev.cellbio.20.022403.093702

Copyright © 2005 by  
Annual Reviews. All rights  
reserved

1081-0706/05/1110-  
0551\$20.00

## Key Words

topographic mapping, Eph receptors, ephrins, mathematical modeling

## Abstract

The sensory and motor components of nervous systems are connected topographically and contain neural maps of the external world. The paradigm for such maps is the precisely ordered wiring of the output cells of the eye to their synaptic targets in the tectum of the midbrain. The retinotectal map is organized in development through the graded activity of Eph receptor tyrosine kinases and their ephrin ligands. These signaling proteins are arrayed in complementary expression gradients along the orthogonal axes of the retina and tectum, and provide both input and recipient cells with Cartesian coordinates that specify their location. Molecular genetic studies in the mouse indicate that these coordinates are interpreted in the context of neuronal competition for termination sites in the tectum. They further suggest that order in the retinotectal map is determined by ratiometric rather than absolute difference comparisons in Eph signaling along the temporal-nasal and dorsal-ventral axes of the eye.

## Contents

INTRODUCTION.....	552
TOPOGRAPHIC MAPPING.....	552
Sensory and Motor Maps.....	553
Auditory Maps.....	553
Visual Maps.....	553
THE RETINOTECTAL MAP AS AN EXPERIMENTAL PARADIGM.....	554
Classical Studies.....	554
The Cell Biology of Mapping ....	555
MODERN IN VIVO STUDIES OF RETINOCOLLICULAR MAPPING.....	560
Development Versus Regeneration	560
Fish Versus Fowl.....	560
Mis/Overexpression in the Chick .	561
Loss-of-Function Studies in the Mouse.....	561
QUANTITATIVE STUDIES.....	565
Gradient Perturbation.....	565
<i>Isl2-EphA3</i> Knock-ins.....	565
A Quantitative Relative Signaling Model.....	568
Computational Approaches.....	574
CONCLUSIONS.....	575

## INTRODUCTION

Vertebrate nervous systems carry multiple, reiterated representations, or maps, of the external world (Kaas 1997). These representations translate stimulus features into a coherent neural code, allowing for the interpretation of what are often complex streams of sensory information. Many maps are organized “topographically” with regard to a stimulus parameter: Auditory neurons that respond to adjacent frequencies, somatosensory neurons that respond to adjacent points on the body surface, and visual system neurons that respond to adjacent points in the visual field are all positioned at adjacent locations within their respective sensory maps. Nervous systems use topographic maps to reduce the

consequences of noise in the transmission of quantized information, to interpolate between data points, and to facilitate the interpretation of coincident stimuli.

How topographic maps are specified and organized during development has been a central preoccupation of neurobiologists for decades. Despite a great deal of effort, it has nonetheless proven difficult to formulate quantitatively rigorous models of map development that can be tested experimentally. Recently, a series of conceptual and experimental advances, derived mainly from molecular genetic analyses, have made this possible for the paradigmatic topographic map: the connection of RGC neurons in the eye to their targets in the optic tectum/SC of the midbrain.

## TOPOGRAPHIC MAPPING

Most topographic maps may be viewed as an ordered array of connections in which the spatial relationships of a set of input neurons are preserved in their synaptic connection to their targets. Frequently, this involves preservation of the Cartesian ( $x,y$ ) positional coordinates within a two-dimensional sheet of sensory neurons—across the surface of the skin, for example—in their connection to a similar two-dimensional sheet of target neurons. Within visual, somatosensory, olfactory, and auditory sensory modalities, multiple such maps are, at successive levels of information processing, repeatedly employed to represent sensory space.

Vertebrate maps are formed over an extended time frame in late embryonic and early postnatal development. In nearly all instances, the process is a dynamic one in which a course initial map is progressively refined into a fine-grained mature map. Map development often begins before the onset of coordinated neuronal activity, shortly after axons initially invade their targets (Holt & Harris 1998, Friauf & Lohman 1999, Rubel & Cramer 2002). Nonetheless, it is now well established that the firing of neurons—spatially correlated within

### RGC (retinal ganglion cell)

**neurons:** the primary output neurons of the eye. RGC axons exit the eye at a single central point (the optic disk) and are bundled together to form the optic nerve

the input ensemble—is crucial for both the progressive refinement and mature precision of topographic maps (Holt & Harris 1993, Debski & Cline 2002). Although we do not discuss the role of correlated electrical activity in map refinement, recent molecular genetic studies have resulted in important advances in this area (e.g., Huh et al. 2000, McLaughlin et al. 2003).

### Sensory and Motor Maps

There are many topographic maps. In the somatosensory system, whose modalities include discriminative touch, pain, temperature, and proprioception, orderly connections are established between peripheral nerve endings and the CNS. In the reciprocal motor system, similarly ordered connections are established between motor neurons in the CNS and neuromuscular junctions in the periphery. Somatotopic organization is thus a hallmark of both input sensory and output motor pathways. The detailed description of this coupled organization by Penfield and colleagues led to the promulgation of the two best-known topographic maps: the cortical maps of the body surface referred to as the motor and somatosensory homunculi, which provide point-to-point cortical representations of the body surface (Penfield & Rasmussen 1950, Kaas 1997).

### Auditory Maps

A second well-known instance of reiterated topographic mapping is seen in the connections that underlie the auditory and vestibular pathways. Auditory connections, for example, are topographic along the low- to high-frequency (distal to proximal) axis of the basilar membrane of the cochlea. These connections encode frequency-specific sound processing and form a “tonotopic” map that is conserved within the anteroventral, posteroventral, and dorsal cochlear nuclei (Echteler & Nofsinger 2000, Rubel & Fritsch 2002). Tonotopy is evident in the projection

of these cochlear nuclei to the superior olivary complex as well as in the inferior colliculus in the midbrain, the medial geniculate nucleus in the auditory thalamus, and the primary auditory cortex in the forebrain. At the level of the inferior colliculus and primary auditory cortex, further topographic connections are made to the SC and the frontal eye field, respectively, where representations of auditory space are integrated (Knudsen 1982, King & Palmer 1983, Cohen & Knudsen 1999).

### Visual Maps

Although this review focuses on a single visual projection—from the retina to the midbrain—topographic mapping is a prominent feature of nearly all the sensory pathways that originate in the eye. Axons from RGCs, the output cells of the retina, exit the eye and fasciculate to form the optic nerve, which enters the brain proper near the ventral hypothalamus. In creatures with forward-facing eyes, roughly half of these axons cross the midline at the optic chiasm and project to the contralateral hemisphere of the brain. (In animals whose eyes are positioned laterally, e.g., mice, nearly all RGC axons make this midline crossing.) As they leave the optic chiasm, retinal axons travel together in the optic tract, which terminates in both the LGN of the thalamus and in the SC of the midbrain (or, in nonmammalian vertebrates, the optic tectum of the midbrain) (Kanaseki & Sprague 1974, Rodieck 1979). Axons from the LGN project to the primary visual (striate) cortex, and from there to a panoply of extrastriate visual areas. Although there is only coarse retinotopic order apparent within the optic nerve, optic tract, and thalamocortical and corticocortical axon tracts in most species, the synaptic terminations of these pathways are precisely retinotopic: The spatial arrangement of RGCs in the retina is preserved in the order of axon terminations in the LGN, the SC, and the striate and extrastriate cortices.

---

**Optic tectum:** a region of the midbrain, one of two primary recipients of RGC input; the other is the lateral geniculate nucleus of the thalamus. In mammals, the optic tectum is referred to as the superior colliculus

**SC:** superior colliculus

**CNS:** central nervous system

**LGN:** lateral geniculate nucleus

---

tn: temporal-nasal

**Chemoaffinity hypothesis:** the idea that the establishment of connections between neurons is directed by “chemical codes under genetic control.” Modern versions of the chemoaffinity hypothesis are predicated on expression gradients of these chemical codes

## THE RETINOTECTAL MAP AS AN EXPERIMENTAL PARADIGM

### Classical Studies

The retinotectal (or retinocollicular) map has been the most intensively analyzed of all topographic maps. Historically, frogs, newts, and fishes have been the favored models for investigating both the configuration of the map and the mechanisms that underlie the map’s formation. The visual responses of these creatures can be assessed using both electrophysiological and behavioral assays, and their optic nerves regenerate following surgical injuries such as transection of the nerve or partial ablation of the retina or tectum. This has allowed investigators to use the regenerating projections of large animals as models for what first occurs in development (Meyer 1982).

In addition to electrophysiology, anatomical methods such as tritiated proline autoradiography, horseradish-peroxidase histochemistry, and focal tectal degeneration following focal ablation of RGCs—pioneered by Sperry and colleagues using the optic system of fishes and amphibians (Attardi & Sperry 1960, Arora & Sperry 1962, Attardi & Sperry 1963)—have been extensively used to study map development. Modern anatomical methods, especially the use of fluorescent axonal tracers such as DiI, have come to dominate studies over the past two decades. At the same time, analyses of the retinotectal projection of chicks and of the equivalent retinocollicular projection of mammals, especially mice, have assumed increasing prominence owing to the considerable interpretive power of gain-of-function studies in the chick and of genetic perturbations, i.e., knockouts and knock-ins, in the mouse. There are important differences in the details of retinotectal mapping in frogs and fishes as opposed to that in mammals (see below), but the basic rules governing map formation now appear to be universal.

**Configuration of the map.** In the retinotectal projection, the Cartesian coordinates

of the eye are mapped onto those of the SC/tectum. Thus, axons that arise from RGCs in the extreme nasal retina (near the nose) project to targets at the far caudal (posterior) end of the SC/tectum; conversely, axons from RGCs in the extreme temporal retina project to the rostral (anterior) end (**Figure 1**). RGCs located at intermediate tn retinal positions project to correspondingly intermediate positions along the rostral-caudal axis of the SC/tectum. The dorsal-ventral axis of the retina, orthogonal to the tn axis, is mapped with equal precision onto the lateral-medial axis of the SC/tectum (**Figure 1**).

**Chemoaffinity.** The dominant model for understanding retinotectal map development has been the chemoaffinity hypothesis promulgated by Sperry (1963). This hypothesis was developed through a series of experiments performed in the regenerating retinotectal projections of amphibians and fish. In one of the best-known experiments, Sperry cut the optic nerves of newts and rotated their eyes 180°. After regeneration of the connection of retinal axons to the tectum, the operated animals behaved as if they saw the world upside down and back to front. Because this response was 180° out of phase with respect to visual experience, it seemed inconsistent with models of retinotectal mapping determined solely by neuronal activity. Sperry postulated that retinal cells carry stable positional chemical labels, or chemoaffinity tags, that determine their proper tectal termination (Sperry 1943, 1944, 1963). He proposed that the simplest configuration of tags, notably with respect to the number of tags required, would occur if the chemical labels took the form of gradients that would mark retinal cells with appropriate  $x,y$  (in his words, “latitude and longitude”) coordinates (Sperry 1963).

**Map perturbations.** Many lines of experiment substantiate the basic concepts in the chemoaffinity model, including the existence of fixed chemoaffinity tags (Fraser & Hunt 1980, Holt & Harris 1993). As

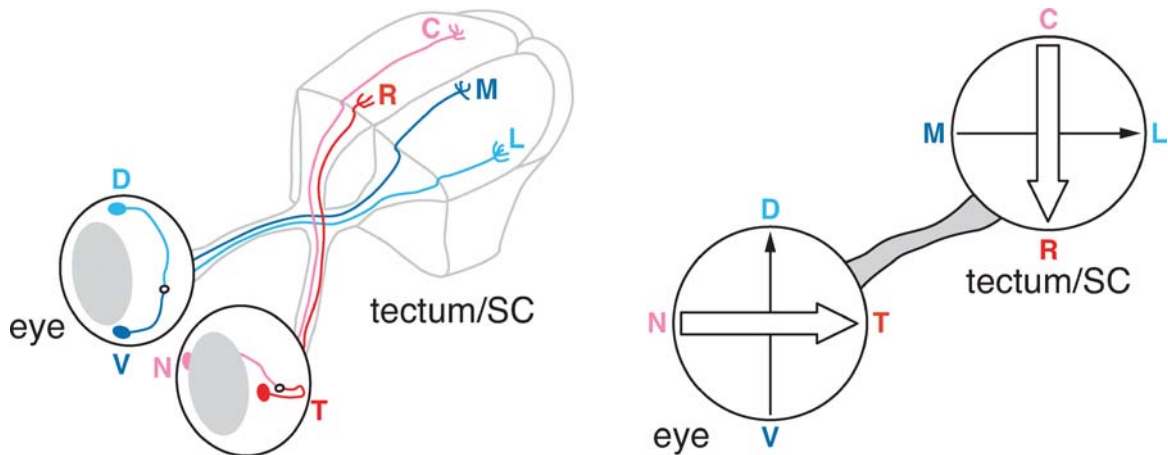


**Figure 1**

Configuration of the retinotectal map. (*Left*) Axonal connections from the eye to the SC, or tectum in nonmammalian vertebrates. As described in the text, the dorsal(D)-ventral(V) axis of the retina is mapped onto the lateral(L)-medial(M) axis of the tectum, and the temporal(T)-nasal(N) axis of the retina is mapped onto the rostral(R)-caudal(C) axis of the tectum. (*Right*) A schematic representation of the map.

noted above, if the optic tectum is rotated after the retinotectal map is mature, the map that regenerates will have nasal RGCs connected to the new rostral end of the rotated tectum. Although experimental phenomena of this sort argued strongly for fixed chemoaffinity labels, many other observations also argued for a considerable measure of plasticity with regard to the expression, stability, or interpretation of these labels. When the nasal half of a retina is ablated, for example, RGC axons from the remaining temporal half sprout, eventually filling the entire tectum. This filling is topographic with respect to position in the remaining retina: The nasal-most remaining RGCs send their axons to the caudal-most tectum (**Figure 2**). This generates an expanded map (Schmidt et al. 1978). Similarly, when the caudal half of the tectum is ablated, retinal axons redistribute to evenly and topographically fill the remaining tectum (**Figure 2**), leading to a compressed map (Sharma 1972, Yoon 1976, Cook 1979). These and related perturbation phenomena led to a great deal of interpretive controversy in the 1970s and 80s not only with regard to the potential plasticity

of positional gradients, but also with respect to the requirement for additional developmental mechanisms that may mediate topographic mapping. Favored among proponents of the latter was the idea that competition among RGC axons for limiting tectal innervation space may, together with chemoaffinity, drive mapping (Prestige & Willshaw 1975). A key problem with regard to deciding between alternative developmental mechanisms was that Sperry's hypothesized chemical labels eluded identification for decades.

## The Cell Biology of Mapping

**Membrane stripe assays and chemorepellents.** In a series of illuminating studies, Bonhoeffer and his colleagues developed and exploited a set of in vitro membrane stripe assays to demonstrate that an important bioactivity guiding the ordered projection of RGC axons along the tn axis of the retina is a chemorepellent that is maximally expressed in the caudal tectum (Walter et al. 1987b). After depositing membrane fractions from rostral and caudal chick tectum in alternating stripes on an in vitro substrate, these workers

---

**Chemorepellant:** an activity (generally a protein) that, unlike a chemoattractant, inhibits axonal growth, extension, and branching, and promotes disintegration of the actin cytoskeleton and growth cone collapse

---

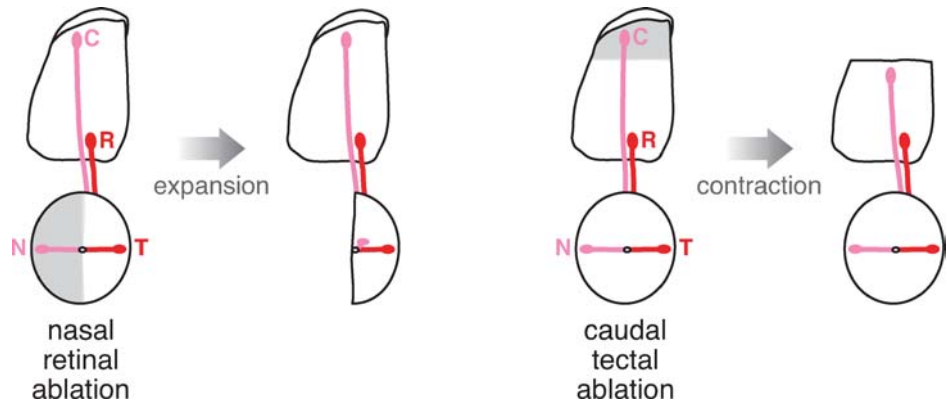


**Figure 2**

Plasticity of the retinotectal map. (*Left*) Map expansion. When the nasal half of the retina is ablated in amphibians, the termination zones of the ablated nasal RGCs are lost from the caudal tectum. The vacated tectal sites are eventually occupied by the axons of the RGCs that remain, and this occupation is retinotopic. (*Right*) Map contraction. When a caudal segment of the tectum is removed, RGC axons redistribute to evenly and topographically fill the tectum that remains.

**GPI:** glycosylphosphatidylinositol

**RAGS:** repulsive axon guidance signal

**Receptor protein-tyrosine kinases:**

transmembrane cell surface receptors, such as the Eph proteins, that contain a protein-tyrosine kinase domain within their cytoplasmic regions

placed explants of nasal or temporal retina orthogonal to these stripes and then observed the frequency and orientation of RGC axonal outgrowth along the stripes. When given a choice, axons arising from RGCs in the temporal retina consistently displayed a strong preference for growth on rostral, as opposed to caudal, tectal membranes (Walter et al. 1987a). In contrast, RGCs in the extreme nasal retina exhibited no strong preference for rostral versus caudal membranes (Walter et al. 1987a, Cox et al. 1990).

Bonhoeffer and colleagues proceeded to show that the chemorepellent activity of the caudal tectal membranes was associated with a protein attached to the membrane surface through a GPI linkage (Stahl et al. 1990, Drescher et al. 1995). They used biochemical fractionation and purification methods to identify and clone cDNAs for one GPI-linked chemorepellent, which they termed RAGS (Drescher et al. 1995). As discussed below, this protein is now referred to as ephrin-A5. It is expressed in concert with the closely related ephrin-A2, which also inhibits axon outgrowth and which is also graded across both the mouse SC and the chick tectum (Cheng

et al. 1995, Drescher et al. 1995, Zhang et al. 1996, Frisén et al. 1998). Given both their graded tectal expression and the principles of chemoaffinity, these caudal tectal chemorepellents were presumed to be sensed by a receptor, or receptors, that would be preferentially expressed in the temporal retina.

**Eph receptors and ephrins.** Studies of retinotectal mapping over the past decade have been greatly stimulated by the identification of the Eph receptors, proteins that were originally isolated from an erythropoietin-producing hepatocellular carcinoma line. The 14 Eph receptors—by far the largest family of receptor protein-tyrosine kinases—are divided in two subfamilies of 8 EphAs (A1–A8) and 6 EphBs (B1–B6). Their ligands, the ephrins, are also divided into two subfamilies, the GPI-anchored ephrin-As (A1–A6) and transmembrane ephrin-Bs (B1–B3).

Interactions of the Eph receptors and their ephrin ligands require cell-cell contact. Indeed, Eph receptors are activated i.e., their protein-tyrosine kinase activity is stimulated, only by multimerized membrane-bound ephrins (or when soluble forms of



ephrins are artificially clustered). In vivo, receptor-ligand engagement invariably occurs at the surface of apposed cells or their processes. EphA receptors bind and are activated by only ephrin-As, and EphBs by only ephrin-Bs, with the exception of EphA4, which binds both ephrin-As and -Bs (Brambilla et al. 1995, Gale et al. 1996). There is considerable promiscuity in ligand-receptor pairing within the A and B subgroups, as measured by in vitro binding assays, although certain features of preferred ligand-receptor pairing within each subgroup have been discerned (Flanagan & Vanderhaegen 1998).

The Eph receptors display structurally distinctive extracellular domains, composed of a ligand-binding globular domain, a cysteine-rich region, and two fibronectin type III repeats. Their cytoplasmic regions are composed of a juxtamembrane domain containing two conserved tyrosine residues, a canonical protein-tyrosine kinase domain, and several protein-protein interaction domains (including a sterile  $\alpha$ -motif and a PDZ-domain binding motif) (Flanagan & Vanderhaegen 1998, Kullander & Klein 2002, Murai & Pasquale 2003).

Depending on cellular context, activation of Eph receptors—as monitored by their autophosphorylation—may lead to either chemorepulsion or chemoattraction. Signal transduction downstream of Eph receptor engagement runs prominently through the small G proteins Rho, Rac, and cdc42 and, in turn, through regulators that directly control the polymerization state of actin. There is evidence for forward and reverse signaling within both the EphA and EphB systems, in that the ephrin-A and ephrin-B “ligands” appear to function as receptors in certain contexts and to signal cell-autonomously (Flanagan & Vanderhaegen 1998, Hindges et al. 2002, Mann et al. 2002). These features of bidirectional signaling and regulation of the actin cytoskeleton have been recently reviewed (Kullander & Klein 2002, Murai & Pasquale 2003). Although there are exceptions (see below), in the context of retinotec-

tal mapping, the preponderance of evidence suggests that forward signaling through Eph receptor-expressing RGCs predominates and that this forward signaling induces chemorepulsion (actin bundling, depolymerization, and growth cone collapse) as a consequence of EphA activation, and chemoattraction (actin polymerization and growth cone extension) as a consequence of EphB activation.

### Gradients of Eph receptors and ephrins.

In RGCs, an EphA3 gradient running from low nasally to high temporally was first reported in the chick; and two favored ligands for EphA3, ephrin-A2 and ephrin-A5, were at the same time found to be expressed in a low-rostral-to-high-caudal gradient in the chick tectum (Cheng et al. 1995, Drescher et al. 1995, Winslow et al. 1995). Both ephrin-A2 and ephrin-A5 are expressed in tectal gradients, but the two ligands display slightly different distributions. In the chick and mouse, ephrin-A2 expression is highest just rostral to the caudal end of the SC/tectum, and decreases smoothly toward the rostral end (Cheng et al. 1995, Zhang et al. 1996, Brennan et al. 1997, Marin et al. 2001). Ephrin-A5 is most highly expressed at the extreme caudal end and decreases more markedly toward the rostral end (Drescher et al. 1995, Monschau et al. 1997). In addition to ephrin-A5 expression in the SC, there is a sharp increase in its expression at the border between the SC and inferior colliculus (Donoghue et al. 1996, Zhang et al. 1996, Hansen et al. 2004).

Mice display a similar low-nasal-to-high-temporal EphA gradient in RGCs (**Figure 3**), but the graded receptors are EphA5 and EphA6, rather than EphA3 (Cheng et al. 1995, Connor et al. 1998, Brown et al. 2000, Marin et al. 2001, Reber et al. 2004). (EphA3 is not expressed by mouse RGCs.) In addition to these graded retinal EphA receptors, there are, in the mouse, chick, and all other species thus far examined, one or more EphA receptors whose expression is ungraded in RGCs along the tn axis (**Figure 3**). EphA4 is expressed but ungraded in the mouse, and both

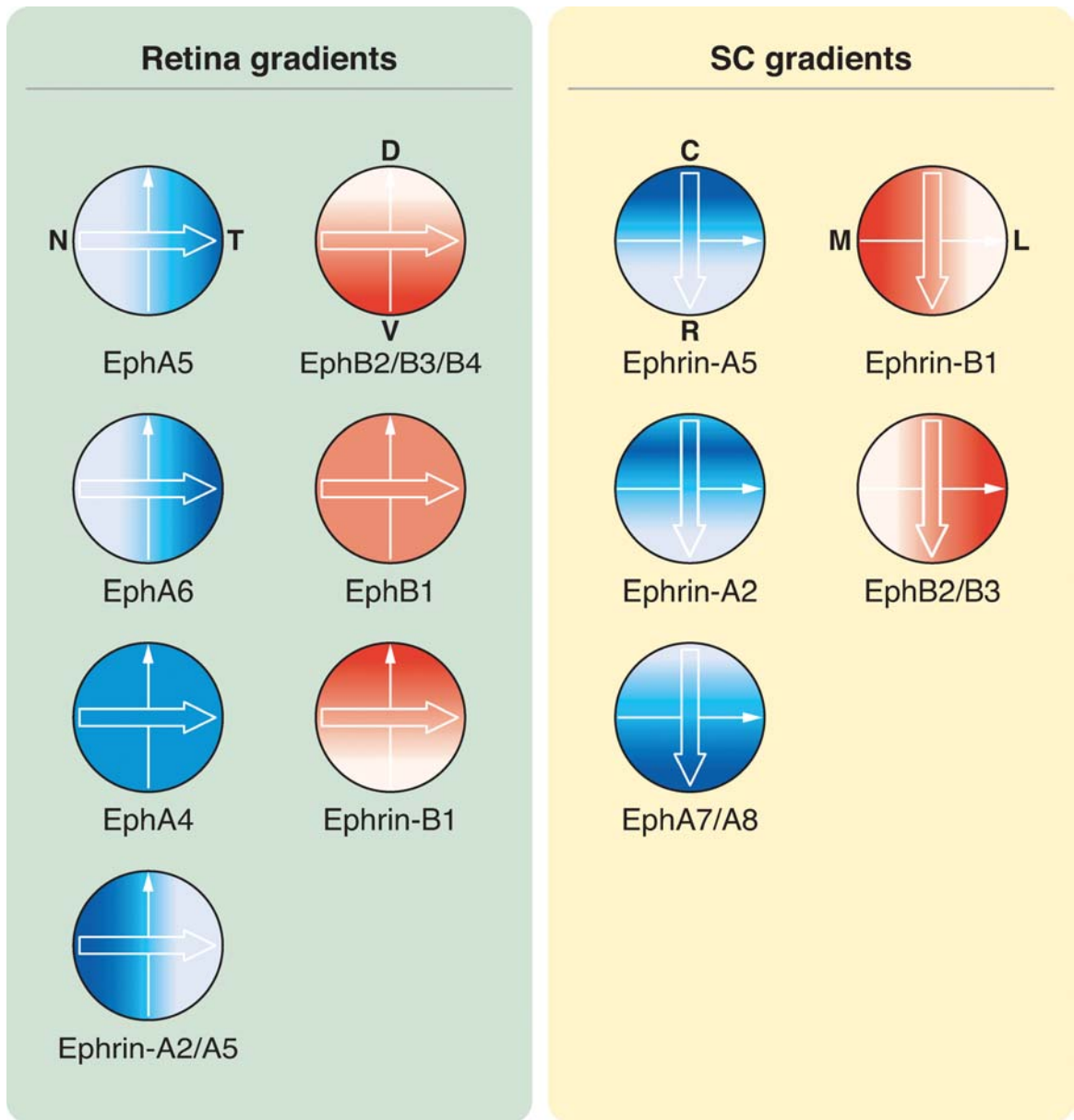


**Figure 3**

Gradients of Ephs and ephrins in the mouse. Retinal gradients (*left set of diagrams*) along the TN axis are depicted in blue, and those along the DV axis are depicted in red. Similarly, collicular gradients (*right set of diagrams*) along the RC axis are depicted in blue, and those along the LM axis are depicted in red. Increasing color indicates increasing expression. Orientation of the retinal and collicular axes are as depicted in **Figure 1** (*right*). Similar gradients exist in other species, although the specific Eph receptor or ephrin ligand that is graded varies between species.



EphA4 and EphA5 are similarly expressed but ungraded in the chick (Marcus et al. 1996, Feldheim et al. 1998, Brown et al. 2000, Reber et al. 2004).

These distributions of receptors and ligands mean that nasal RGCs that have the fewest EphA receptors project to caudal tectal (collicular) targets with the highest levels of ephrin-As and, conversely, that temporal RGCs with the most EphAs project to rostral targets that contain the lowest levels of ephrin-As. This pattern is in keeping with the finding that the GPI-linked ephrin-As are chemorepellents for EphA-expressing axons and with *in vitro* observations that temporal RGCs, which carry the highest levels of EphA, are the most sensitive to the GPI-linked chemorepellent activity of the caudal tectum.

The orthogonal axes of the retinotectal projection—the dorsal-ventral axis of the retina and the lateral-medial axis of the SC/tectum—have received less experimental attention but have not been neglected. Eph proteins and their ligands are also distributed in gradients along these axes, but it is the EphBs and the ephrin-Bs that form these gradients, rather than the EphAs and ephrin-As (**Figure 3**). EphB2, EphB3, and EphB4 are each expressed in a high-ventral-to-low-dorsal gradient in the retina (Holash & Pasquale 1995, Henkemeyer et al. 1996, Connor et al. 1998, Birgbauer et al. 2000, Hindges et al. 2002), and ephrin-B1 is present in a high-medial-to-low-lateral gradient in the mouse SC/tectum (Braisted et al. 1997, Hindges et al. 2002). These gradients mean that ventral RGCs with the most EphBs project to medial collicular targets where ephrin-B levels are highest, the exact opposite of the situation with the EphAs/ephrin-As on the orthogonal axes. This configuration of EphB/ephrin-B gradients led workers to speculate that forward signaling through EphBs in RGCs would result in chemoattraction, rather than chemorepulsion, during retinotectal mapping. This possibility has recently been tested experimentally (see below).

Just to make things more complicated, Eph proteins—both EphAs and EphBs—are also expressed in gradients in the SC/tectum, and ephrins—both ephrin-As and ephrin-Bs—are also expressed in gradients in the retina (Marcus et al. 1996, Brennan et al. 1997, Connor et al. 1998, Hornberger et al. 1999, Marin et al. 2001, Menzel et al. 2001, Hindges et al. 2002). In general, the gradient of a given ligand or receptor runs counter to that of its cognate receptor or ligand (**Figure 3**). Thus, in the chick retina, ephrin-A2, -A5, and -A6 are expressed in a high-nasal-to-low-temporal RGC gradient, counter to the gradient of EphA3 (Connor et al. 1998, Hornberger et al. 1999, Menzel et al. 2001). In the chick tectum, EphA3 and EphA5 are expressed in a high-rostral-to-low-caudal gradient, counter to the gradient of ephrin-A2 and -A5 (Connor et al. 1998, Marin et al. 2001). Similarly, ephrin-A2 and -A5 have been detected in a high-nasal-to-low-temporal gradient in the mouse retina (Gale et al. 1996, Marcus et al. 1996, Brennan et al. 1997, Monschau et al. 1997), and EphA7 and EphA8 have been found in high-rostral-to-low-caudal collicular gradients (Park et al. 1997, Rogers et al. 1999, Knoll et al. 2001). In the mouse retina, ephrin-B1 and -B2 are expressed in a high-dorsal-to-low-ventral RGC gradient (Marcus et al. 1996, Birgbauer et al. 2000, Hindges et al. 2002), and EphB2 and B3 are expressed in a high-lateral-to-low-medial gradient in the SC (Hindges et al. 2002).

These Eph/ephrin countergradients cannot be ignored as they are also seen in other regions in the developing CNS. However, their biological significance is at present unresolved and they remain the subject of active study. There are several alternative hypotheses as to the role of ephrins in the retina and Eph receptors in the SC/tectum (Connor et al. 1998, Hornberger et al. 1999, McLaughlin & O'Leary 1999, Menzel et al. 2001, Yates et al. 2001). These include the idea that retinal ephrin-As (a) serve to “shape” the retinal EphA gradient by binding to EphA4 locally in the nasal retina and inhibiting EphA4 action in the tectum, (b) are transported along RGC

---

**TZs:** termination zones

---

axons to the SC/tectum where they might function in map refinement, or (c) may mediate “reverse-signaling” events in both locations. Some of these possibilities are discussed in the context of the molecular genetic experiments summarized below.

**Chemorepellent activity of ephrin-As.** As noted above, most studies of retinotectal mapping have focused on the tn to rostral-caudal projection. In this projection, forward signaling mediated by chemorepellents in the tectum appears to dominate. These chemorepellents are ephrin-A2 and -A5. In *in vitro* membrane stripe assays, they mediate the selective outgrowth of temporal axons onto rostral membranes as well as the selective sprouting of collateral axon branches that arise from a primary axon shaft (Walter et al. 1987a, Godement & Bonhoeffer 1989, Roskies & O’Leary 1994). Axons from temporal RGCs are strongly repelled by both ephrin-A5 and ephrin-A2 in the stripe assays. Ephrin-A5 also shows weak chemorepellent activity against nasal axons (Drescher et al. 1995, Monschau et al. 1997). Collateral axon-branch formation, the primary mechanism of topographic map development in higher vertebrates (Yates et al. 2001, Sakurai et al. 2002), is also inhibited by caudal collicular membranes and ephrin-As in these assays (Roskies & O’Leary 1994).

## MODERN IN VIVO STUDIES OF RETINOCOLLICULAR MAPPING

### Development Versus Regeneration

As noted above, the pioneering work on retinotectal map development was performed in young adult fish or amphibians, following nerve injuries or tissue displacements. But in these creatures, the retinotectal system continues to develop late into adult life. As they grow, their retinae and tecta also grow: Retinal cells are added at the periphery of the eye, and tectal cells are added at the caudal-medial edge of the target. Therefore, most of the clas-

sical mapping studies are in fact compound experiments that include both regeneration and *de novo* development, with regrown fibers and newly innervating fibers intermixed in the tectum. Active fiber guidance, involving axon-axon interactions between these fiber populations, is an important mechanism for regenerating retinotectal axons in these settings (Gaze & Fawcett 1983, Taylor & Gaze 1985). Regeneration studies therefore have limitations with regard to addressing map formation as it first occurs in development.

### Fish Versus Fowl

More recent studies of initial retinotectal development in frogs (Holt & Harris 1983, Holt 1984, Sakaguchi & Murphey 1985) and fish (Stuermer 1988) indicate that topographic order is in fact present at early stages of development, with the growth cones of retinal axons reaching their topographically correct regions in the tectum with relatively high initial fidelity. That is, navigation of the tectal surface as well as the decision as to where a particular RGC should terminate and arborize appear to be executed by the growth cones of RGCs in frogs and fish. Eventual TZs are established and refined through the extension of many small branches at the base of the growth cone in a process termed “backbranching.”

This situation with respect to frogs and fish appears to be superficially different from that of chicks and rodents, where the axonal growth cone plays essentially no role in deciding where a particular RGC should terminate. However, this difference may be deceptive. Studies of the development of retinotectal projections in chick (Nakamura & O’Leary 1989, Yates et al. 2001) and of retinocollicular projections in rat (Simon & O’Leary 1992a–c) and mouse (Hindges et al. 2002) demonstrate that primary RGC axons at first significantly overshoot their correct TZs along the rostral-caudal axis of the SC/tectum and that axon distribution along the medial-lateral axis is also initially diffuse. Indeed, the growth cones of most RGC axons—irrespective of where they

arise along the tn axis of the retina—initially run all the way to the caudal end of the tectum/SC. Later on, these axons extend interstitial collateral axons branches, which over time become increasingly concentrated at the correct TZ. Collateral branches outside the TZs are less and less frequently observed as development proceeds and the primary axon shaft is eventually retracted to a tightly circumscribed TZ (Nakamura & O’Leary 1989, Simon & O’Leary 1992, Yates et al. 2001, Hindges et al. 2002). This process of branching, refinement, retraction, and consolidation takes place over the first postnatal week in mouse and by P8 the map resembles its mature form. The differences in map refinement between frogs and fish on the one hand and chicks and rodents on the other—particularly with respect to the role of the growth cone as a tectal sensor—may be more apparent than real. The rostral-caudal extent of the tectum is vastly (~50-fold) larger in the chick than the frog at the onset of mapping. The fraction of the total tectal surface that may be sampled by a single growth is therefore corresponding very much larger in the frog (McLaughlin et al. 2003). And from a cell biological perspective, the extensive and dynamic backbranching seen at the base of amphibian growth cones is essentially the same process of biased actin polymerization seen in the collateral axon branching of higher vertebrates. Eph/ephrin signaling regulates both.

### Mis/Overexpression in the Chick

Gain-of-function studies were among the first to substantiate a chemorepellent role for ephrins in retinotectal mapping in vivo (Nakamoto et al. 1996). In these experiments, patches of exogenous ephrin-A2 were produced in the developing chick tectum through infection of embryos with a retrovirus that contained an ephrin-A2 cDNA. Via this manipulation, ephrin-A2 patches were superimposed in a random pattern on top of the gradient of endogenous ephrin-A2 and -A5. Small numbers of both mid-temporal and nasal

RGC axons, labeled by focal injection of DiI into the contralateral retina, were then monitored for their mapping behavior around, in, or through these ectopic ephrin-A2 patches. Mid-temporal axons, which express relatively high levels of EphA receptors and are particularly sensitive to the membrane-associated chemorepellent of the caudal tectum, were observed to avoid the patches and to map to rostrally shifted tectal sites. In contrast, axons from RGCs in the extreme nasal retina, which normally have a limited ability to distinguish between rostral and caudal tectal membranes, did not (Nakamoto et al. 1996).

More recently, the role of ephrin-B1 was also assessed by gain-of-function studies in the chick (McLaughlin et al. 2003). Tectal electroporation of a retrovirus carrying an ephrin-B1 cDNA again generated patches of high ephrin-B1 expression superimposed onto the endogenous ephrin-B1 gradient. These studies demonstrated that collateral branches arising from primary axons located laterally to their correct termination site were attracted up the ephrin-B1 gradient to medially positioned ephrin-B1 patches. Conversely, branches arising from axons medial to their termination site were repelled down the ephrin-B1 gradient to laterally positioned patches. Together with the results of *EphB2/B3* knockout studies (see below), these findings have been interpreted as indicative of a bifunctional role of ephrin-B1 as both a branch repellent and attractant in the control of mapping along the lateral-medial axis of the tectum. However, the biochemical mechanisms that may underlie such bidirectionality remain obscure (McLaughlin et al. 2003).

### Loss-of-Function Studies in the Mouse

***Ephrin-A5* knockouts.** Frisen and colleagues (1998) studied the role of ephrin-A5 in vivo by generating knockout mice that lack this ligand. In these mice, retinal axons establish TZs at topographically incorrect sites (**Figure 4**). Some axons initially overshoot the

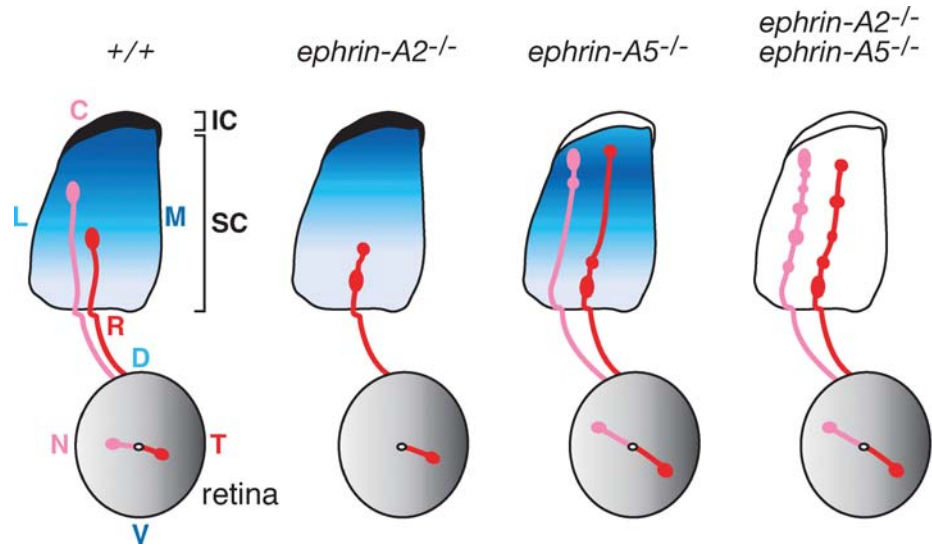


**Figure 4**

Mapping anomalies in mouse *ephrin-A* knockouts (*three right panels*) versus wild type (+/+, *first panel*). In *ephrin-A2* mutants (*second panel*), temporal RGCs terminate in their normal rostral position, but also sometimes in a second, more caudally positioned TZ. In *ephrin-A5* knockouts (*third panel*), temporal RGCs display similar mismapping phenomena, occasionally accompanied by a TZ in the far caudal SC. Nasal RGCs sometimes terminate in additional ectopic TZs that are positioned rostrally to their appropriate site. In mice lacking both *ephrin-A*s (*fourth panel*), multiple TZs, arrayed all along the rc axis of the SC, are seen following DiI injections into either the nasal or temporal retina. Perturbations in *ephrin-A* gradients are depicted only for the SC, although as discussed in the text, these gradients are also lost from the retina in the knockouts. Gray shading in the retina depicts the aggregate EphA gradient in the mouse.

SC and make connections in the inferior colliculus. This suggests that the sharp increase in *ephrin-A5* seen at the border between the SC and the inferior colliculus is important in the delimitation of this border. Other retinal axons transiently overshoot their correct TZ but remain in the caudal SC. Aberrant TZs are less prevalent in the middle of the SC's rostral-caudal axis, where *ephrin-A2* is most highly expressed. Frisen and colleagues suggest that ectopic TZs in the caudal SC may be accounted for by the fact that the low level of *ephrin-A2* present in this region is incapable (in the absence of *ephrin-A5*) of inhibiting the inappropriate branching of mid-temporal axons in the caudal SC.

***Ephrin-A2/-A5* double knockouts.** Analysis of double mutants that lack both *ephrin-A2* and *-A5* dramatically demonstrate

that their repellent activity is required for normal retinocollicular mapping (Feldheim et al. 2000). These double knockouts display marked abnormalities in the retinocollicular projection. Topographic mapping from the tn axis of the eye to the rostral-caudal axis of SC is almost entirely lost (**Figure 4**). RGCs from both nasal and temporal retinal locations are seen to terminate at multiple sites all along the rostral-caudal axis of the SC. The magnitude and extent of mapping anomalies in the double mutants is very much larger than in either the *ephrin-A2* or *ephrin-A5* single knockouts, consistent with complementary and overlapping roles for these *ephrin-A*s in mapping (Feldheim et al. 2000).

The mapping abnormalities of the *ephrin-A2/-A5* double mutants are most straightforwardly explained by the nearly total loss of chemorepellent activity in the SC,

although an important complication of any standard knockout analysis is that the gene in question is inactivated everywhere in the organism. Thus, the normal high-nasal-to-low-temporal ephrin-A gradient in the retina is also eliminated in the double mutants. Feldheim and colleagues (2000) addressed this issue with “mix-and-match” in vitro membrane stripe assays in which RGCs from either mutant or wild-type retina were confronted with alternating stripes of rostral and caudal collicular membranes from either mutant or wild-type mice. Axons from wild-type temporal RGCs showed no preference for rostral versus caudal membranes when confronted with membranes prepared from the double mutants, consistent with the loss of topographic mapping being accounted for by a loss of chemorepellent activity in the target. However, a modest increase in the sensitivity of nasal double-mutant RGCs to chemorepulsion by caudal wild-type membranes was also noted in these in vitro assays. This finding in turn is consistent with the idea that the ephrin-As preferentially expressed in the nasal retina normally may dampen, through the retinal engagement of EphAs, the ability of nasal RGCs to use these EphAs to sense ephrin-As in the target (Connor et al. 1998, Dutting et al. 1999, Hornberger et al. 1999).

***EphA5* knockouts.** Loss-of-function analyses have also been reported for the mouse *EphA5* gene (Feldheim et al. 2004). Mapping abnormalities are only partially penetrant in these mutants. For example, approximately 50% of temporal RGCs project normally, with the remaining 50% displaying both a normal TZ and in addition one or more ectopic, caudally displaced TZs (Figure 5). This partial penetrance of the *EphA5* mutant phenotype is not unexpected, given that the retinal EphA gradient in the mouse is generated by three receptors: two that are graded (EphA5 and EphA6) and one that is not (EphA4). In general, the misprojections evident in the EphA5 mutant mice

are entirely consistent with the EphA5 receptor making a significant contribution to the ability of temporal RGCs to sense the ephrin-A chemorepellents that are maximally expressed in the caudal SC. Mix-and-match in vitro membrane stripe assays, similar to those performed for the *ephrin-A2/-A5* double knockouts, also support the conclusions that EphA5 acts primarily as a forward-signaling receptor in temporal RGCs and is necessary for these neurons to respond fully to ephrin-A chemorepellents in the SC (Feldheim et al. 2004).

***EphB2/B3* double knockouts.** Hindges and colleagues used double knockouts of the mouse *EphB2* and *EphB3* genes to address the role of EphB receptors in the mapping of the dorsal-ventral axis of the retina to the lateral-medial axis of the SC (Hindges et al. 2002). As noted above, the gradients of EphB2 and EphB3 (from low-dorsal-to-high-ventral in the retina) and of ephrin-B1 (from low-lateral-to-high-medial in the SC)—assuming that ephrin-Bs are chemoattractants—are consistent with such a role. Conventional mouse mutants lacking the EphB2 and EphB3 proteins entirely, as well as an EphB2 mutant with intact extracellular and transmembrane domains but without a tyrosine kinase domain, were employed. In the latter mutant protein, designated EphB2ki, the EphB2 kinase domain is replaced with  $\beta$ -galactosidase. This mutant protein therefore retains the capacity for reverse signaling but loses the capacity for forward signaling.

Analyses of the retinocollicular maps in these mutants demonstrated an important role for EphB2 and EphB3 forward signaling in topographic mapping, notably with regard to the medial-lateral collicular orientation of the interstitial branches that are extended from the primary shafts of RGC axons during map formation (Hindges et al. 2002). Ectopic, laterally shifted TZs were frequently observed along the medial-lateral axis of the SC in the *EphB2/B3* double mutants but



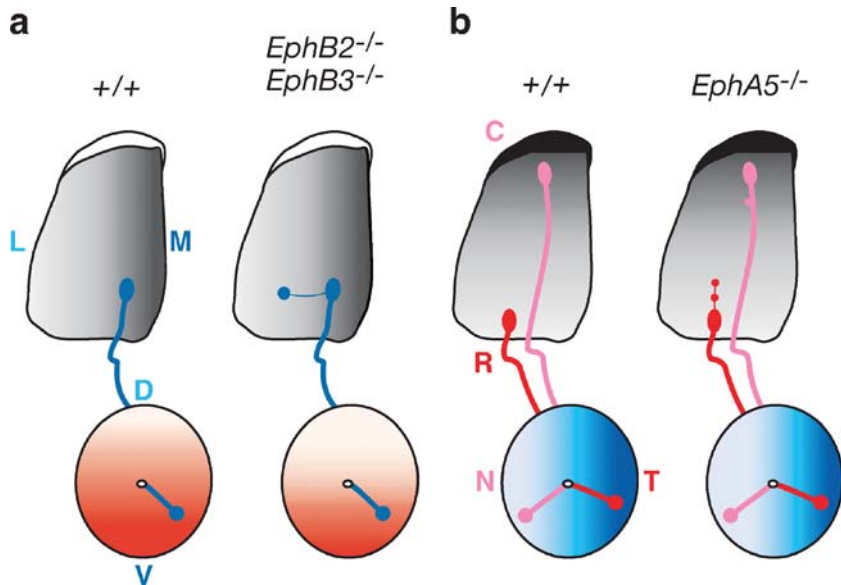


**Figure 5**

Mapping anomalies in mouse *EphB2/B3* double knockouts (*a*, second panel) and *EphA5* knockouts (*b*, fourth panel) versus wild type (*first and third panels*). In the *EphB2/B3* mutants, ventral-temporal RGCs project to a normal medial-rostral TZ in the SC and occasionally also to an abnormal, more lateral TZ (*second panel*). In the *EphA5* mutants, temporal RGCs project to their normal sites in the rostral SC and occasionally to more caudal TZs (*fourth panel*). Nasal *EphA5*<sup>-/-</sup> RGCs occasionally display abnormal, rostrally positioned TZs, a phenotype that may be secondary to the development of ectopic caudally positioned TZs from temporal RGCs. Perturbations in EphB and EphA gradients are depicted only for the retina although, as discussed in the text, gradients are also lost from the SC in the knockouts. Gray shading in the SC depicts the aggregate gradients of ephrin-Bs (*a panels*) and ephrin-As (*b panels*) in the mouse.

rarely observed along the rostral-caudal axis (**Figure 5**). These laterally shifted TZs were always observed in addition to a correctly positioned TZ, and their appearance was, as for the *EphA5* mutants, not fully penetrant. This is again to be expected because, in addition to EphB2 and EphB3, EphB1 and EphB4 are also expressed in the mouse retina (Birgbauer et al. 2000, Hindges et al. 2002). Importantly, Hindges and colleagues demonstrated that the lateralization of mature TZs is accounted for by a perturbation of interstitial axon branching; the propensity for these branches to be oriented laterally (relative to the main axon shaft) increased significantly in the double mutants (Hindges et al. 2002; **Figure 5**). This disruption was even more pronounced in the *EphB2ki/B3* double mu-

tants than in the *EphB2/B3* double mutants. This suggests that the kinase inactive receptor may have a dominant-negative effect and, more importantly, demonstrates that EphB forward signaling (i.e., signaling in the receptor-expressing RGCs) is the dominant signaling pathway for regulation of the formation and orientation of interstitial branches along the medial-lateral axis. Given the distribution of EphBs in the retina and ephrin-Bs in the SC, these results suggest that EphB signaling promotes branch extension up the ephrin-B gradient. It is important to note that some medially oriented axon branches are still observed in the *EphB2/B3* double mutants and that evidence for reverse signaling through ephrin-Bs expressed by dorsal RGCs has been presented in *Xenopus* (Mann et al.



2002). Thus, additional mechanisms, perhaps involving a collicular chemorepellent activity distributed in a lateral-medial gradient similar to that of ephrin-B1, probably operate during topographic mapping.

## QUANTITATIVE STUDIES

### Gradient Perturbation

The hypothesis that gradients of Eph receptors and ephrins regulate topographic mapping is representative of a class of developmental models in which cells are ordered and distinguished from one another not by all-or-none differences in gene expression but rather by graded differences. As a means of testing such models, conventional loss-of-function analyses may provide a qualitative assessment of the importance of a particular signaling system. Such analyses, however, are limited with respect to providing a mechanistic understanding of the system. For example, the case for another candidate regulator of retinotectal mapping—RGM (Monnier et al. 2002)—was weakened when mouse knockouts of the RGM gene were found to display normal retinocollicular maps (Niederkofler et al. 2004). And conversely, the nearly complete loss of normal topography observed in the *ephrin-A2/-A5* double knockouts (Feldheim et al. 2000) greatly strengthens the case for EphA signaling playing a central role in retinocollicular mapping. However, such knockouts provide only a qualitative test of what is a quantitative model and do not yield direct insights into whether mapping actually requires the continuously graded expression of ligands and receptors. Such an assessment can only be made if the gradients in question are perturbed in a systematic and informative way. In the retinotectal system, this would require changing the slope, the shape, the orientation, or the periodicity of either the Eph receptor or ephrin ligand gradients in a quantifiable way such that predictions as to alterations in topographic mapping can be made and tested. This has been carried out in a set of

knock-in and compound mutant mice (Brown et al. 2000, Reber et al. 2004).

### *Isl2-EphA3* Knock-ins

Perturbation of the EphA gradient in the mouse retina was achieved through the ectopic expression of EphA3 in a subset of RGCs (Brown et al. 2000). Although not expressed in mouse RGCs, EphA3, like EphA5 and EphA6, binds the collicular ephrin-A ligands with high affinity. A mouse EphA3 cDNA was inserted into the 3' untranslated region of the mouse *Isl2* (*Isl2*) gene downstream of a viral internal ribosome entry site sequence. This construct brings EphA3 under the control of the regulatory elements of the *Isl2* gene but does not perturb endogenous *Isl2* expression. *Isl2* is expressed at a constant level in a subset (~40%) of RGCs that are randomly scattered across the retina in a salt-and-pepper fashion (except for the extreme ventral-temporal crescent of the retina, where the number of *Isl2*<sup>+</sup> cells is lower). Importantly, the *Isl2* gene is not expressed in the SC. Any perturbations of retinocollicular mapping are therefore specific to the retina (Brown et al. 2000). The *Isl2-EphA3* construct was “knocked-in” to the mouse *Isl2* locus through homologous recombination in embryonic stem cells (Brown et al. 2000).

**Map duplication and collapse.** A mixed population of RGCs was thereby generated in the mice produced from these cells. One of these RGC populations is wild type and carries the endogenous smooth gradient of EphA receptors; the other population has “spikes” of new EphA3 expression superimposed on top of this gradient (**Figure 6**). This generates a compound gradient that is quasi-oscillatory, with the oscillations—the EphA3 spikes—having twice the amplitude in *Isl2-EphA3* homozygotes as in heterozygotes. Brown et al. (2000) analyzed the retinocollicular maps in these knock-in mice relative to wild type by first making small focal injections of DiI into the retina and then plotting the

---

**RGM:** repulsive guidance molecule

---

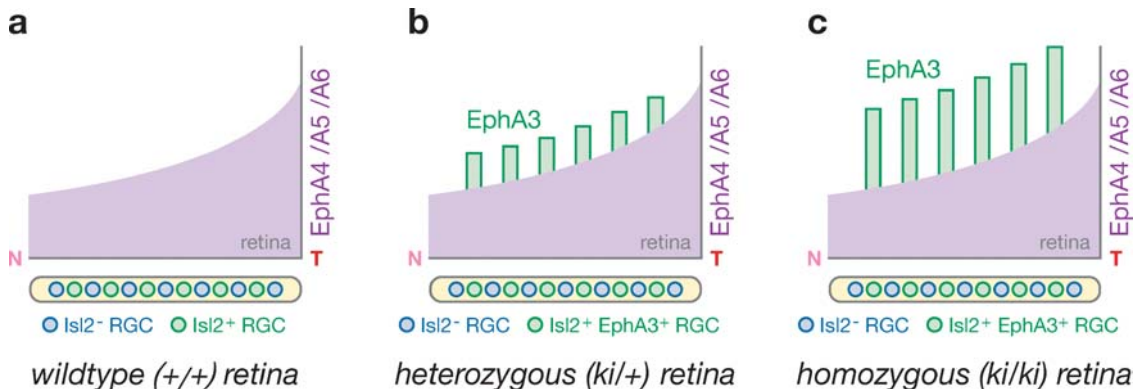


**Figure 6**

Systematic perturbation of the retinal EphA gradient in *Isl2-EphA3* knock-in mice. (a) The aggregate EphA gradient in wild-type mice increases smoothly from the nasal (N) to the temporal (T) end of the retina. This aggregate gradient is composed of two receptors (EphA5 and EphA6) whose expression varies and one (EphA4) whose expression does not. RGCs that express the transcription factor Islet-2 (*Isl2*<sup>+</sup>, green circles) and RGCs that do not (*Isl2*<sup>-</sup>, blue circles) both contribute to the gradient. (b) The aggregate EphA gradient in mice heterozygous for the *Isl2-EphA3* knock-in. This gradient is now quasi-oscillatory and has constant but intermittent “spikes” of ectopic EphA3 expression—contributed by *Isl2*<sup>+</sup> RGCs—superimposed onto the normal aggregate EphA gradient. (c) The aggregate EphA gradient in mice homozygous for the *Isl2-EphA3* knock-in is the same as that for the heterozygous knock-ins except that the EphA3 spikes are twice as large. Modified from Brown et al. (2000), with permission.

position of these injections along the tn axis relative to the number and position of the TZs labeled (after 24 hours) in the contralateral SC (Figure 7).

These retinocollicular maps turned out to be especially informative. The wild-type mouse map is an apparently linear transfer of the retinal tn axis onto the collicular rostral-caudal axis (Figure 7). In marked contrast, *Isl2-EphA3* homozygotes display two maps rather than one. Thus, for each retinal location, single extracellular DiI injections into the retina—which always label a population of normal RGCs as well as an immediately adjacent population of EphA3<sup>+</sup> RGCs—yield two TZs in the SC rather than one (Brown et al. 2000). This means that the retinocollicular map is effectively duplicated: Every point in visual space along the tn axis of the eye is represented at two different locations in the SC. Brown et al. (2000) demonstrated that the more caudal of these TZs corresponds exclusively to wild-type RGCs and the more rostral to EphA3<sup>+</sup> RGCs. This is as ex-

pected because the EphA3<sup>+</sup> cells have higher summed EphA levels and therefore should be more sensitive to the chemorepellent activity of the rostral-to-caudal collicular ephrin-A gradient.

Perhaps most importantly, neither of the retinocollicular maps of the homozygous *Isl2-EphA3* knock-ins is normal: The wild-type map does not take its wild-type form but rather is displaced caudally in the SC as a result of the preferential occupation of the rostral SC by EphA3<sup>+</sup> RGCs (Figure 7). This observation alone provides strong *in vivo* evidence for the hypothesis, debated for decades, that RGCs compete with one another as an ensemble for innervation space in the SC. It also demonstrates that RGCs do not terminate in the SC on the basis of a fixed or absolute level of EphA signaling but rather on the basis of an ensemble-wide comparison tied to relative levels of EphA signaling.

The retinocollicular map of the *Isl2-EphA3* heterozygotes displays two features that are distinct from the homozygote map. Like the

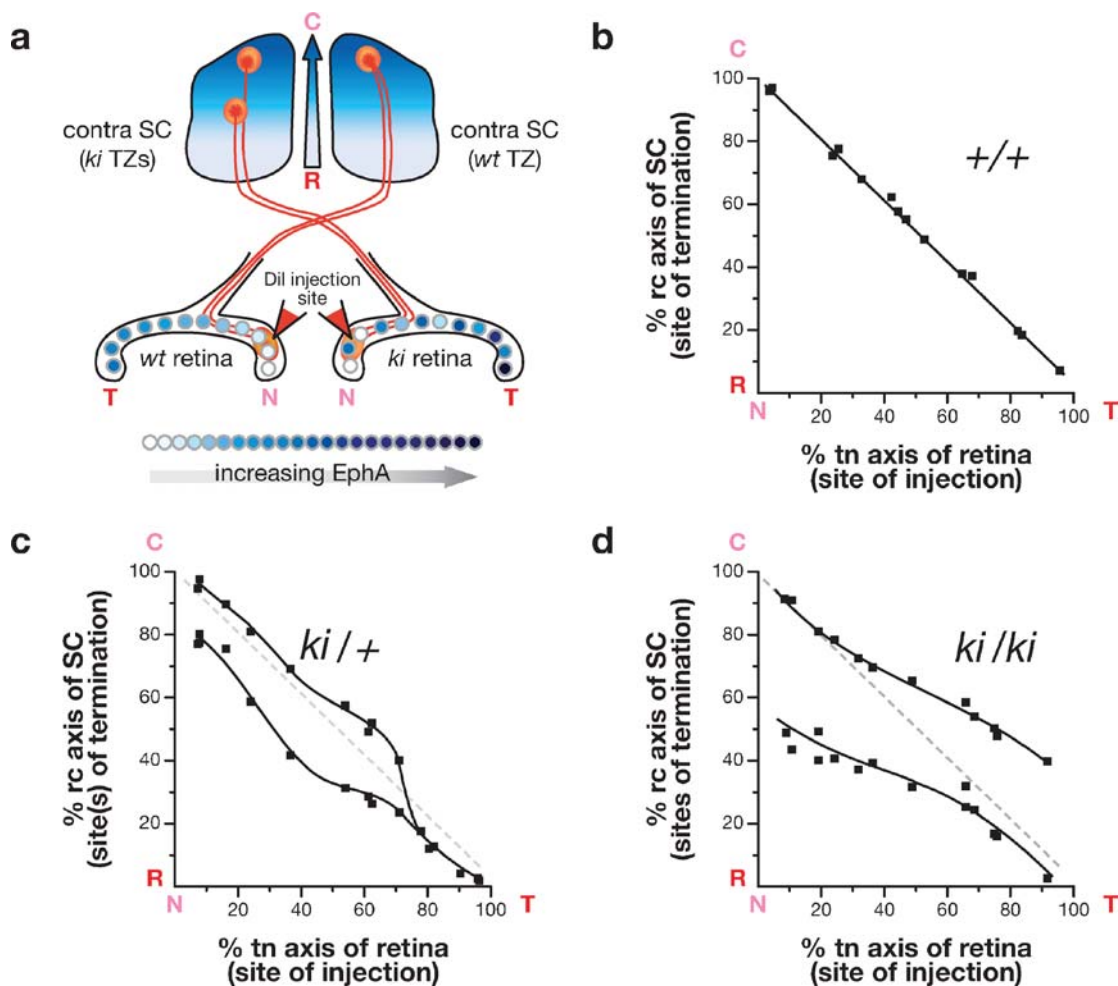


**Figure 7**

Retinocollicular maps in the *Lsl2-EphA3* knock-ins. (a) Focal injection of DiI into the nasal retina of wild-type (*wt*, left) versus knock-in (*ki*, right) mice labels small clusters of cells. Adjacent wt RGCs with equivalent EphA project to one TZ in the caudal SC whereas adjacent ki RGCs with different levels of EphA project to two TZs, the more rostral of which corresponds to *EphA3*<sup>+</sup> RGCs. (b) The retinocollicular map of wild-type mice. The x axis is the tn axis of the retina (N = 0, T = 100) and the y axis is the rostral-caudal axis of the SC (R = 0, C = 100). Plotted is the rostral-caudal center of each DiI-labeled TZ as a function of the tn position of the retinal injection through which that TZ was labeled. (c) The retinocollicular map of *Lsl2-EphA3* heterozygotes. DiI injections performed over the first 76% of the retinal tn axis always yield two TZs (as schematized in a), rather than one, whereas all injections performed over the remaining 24% of the axis always yield a single TZ. This results in partial map duplication and collapse. (d) The retinocollicular map of *Lsl2-EphA3* homozygotes. DiI injections performed over the full retinal tn axis always yield two TZs rather than one. Dashed gray lines in c and d mark the wild-type map. Modified from Brown et al. (2000), with permission.

homozygote map, the retinocollicular map is duplicated but only for the nasal-most 76% of the retinal tn axis (where nasal = 0%, and temporal = 100%). All DiI injections performed in more temporal regions of the retina—from 76% to 100% of the tn axis—yield only a single TZ. Brown and colleagues refer to this as mapping “collapse,” because the map changes suddenly from a duplicated to a single map. In addition, in the nasal-most 76% of the retina where the heterozygote map is duplicated, the extent of the duplication—that is, the separation between EphA3<sup>-</sup> and EphA3<sup>+</sup> TZs arising from each retinal location—is on average half that seen in homozygous *Isl2-EphA3* knock-ins.

**Relativity in EphA signaling.** These retinocollicular maps are not consistent with simple mass-action models of topographic mapping that are based on ligand-receptor matching or on topography being determined by a fixed value of EphA signaling (Nakamoto et al. 1996). Instead, order of termination within the SC appears to be determined by relative EphA levels, that is, the level of EphA signaling in a given RGC relative to that in all other RGCs. Thus, all temporal EphA3<sup>+</sup> RGCs still project to the SC in the knock-ins in spite of the fact that they have a much higher level of EphA receptors than does any wild-type RGC. Independent of their absolute level of EphA expression, axons with the highest EphA level always project to the most rostral site. Moreover, two RGCs located at the opposite end of the tn axis of the retina will project to the very same rostral-caudal position in the SC if they express the same level of EphA.

### A Quantitative Relative Signaling Model

**Exponential gradients.** Reber and colleagues (2004) noted that these observations are most economically explained by a devel-

opmental program in which RGCs compete as an ensemble for termination sites along the rostral-caudal axis of the SC through comparison of relative, or ratio-based, differences in EphA signaling intensity—a program in which RGCs are ordered on the basis of a fold-difference in aggregate EphA ( $\Sigma$ EphA) signaling between themselves and all of their competitors. Reber et al. termed this ratiometric comparison “relative signaling.” If such a comparison is in fact made, and if  $\Sigma$ EphA signaling intensity is proportional to  $\Sigma$ EphA expression, then the apparent linearity of the wild-type retinocollicular map (**Figure 6**) requires that, for the EphA receptors that vary (in the mouse EphA5 and EphA6), the rate of change in the concentration of these receptors per RGC (designated  $C_v$ ) along the tn axis of the retina must be proportional to the receptor concentration itself (Reber et al. 2004). If the retinal axis is designated the  $x$  axis, then this is expressed as

$$\begin{aligned} dC_v &= kC_v dx \\ \text{or } C_v(x) &= C_{v0}e^{kx}, \end{aligned}$$

where  $k$  is a constant and  $C_{v0}$  is the value of  $C_v$  at  $x = 0$ , the nasal pole of the retina. (In the studies of Brown et al. (2000) and Reber et al. (2004), the temporal pole is assigned the value 100.) Because there is also an ungraded EphA receptor in the mouse (EphA4), the full aggregate EphA receptor distribution ( $C$ ) should be described by an exponential plus a constant ( $C_4$ ), i.e.,

$$C(x) = C_{v0}e^{kx} + C_4$$

(Reber et al. 2004). Accurate quantitation of EphA receptor protein levels as a function of position across the tn axis of the retina is rendered problematic, if not impossible, by two considerations. The more important of these is that the receptor proteins do not remain in RGC cell bodies. Instead, they are transported down RGC axons, which are both bundled together in the retina and, at the start of mapping, highly intermixed in the SC (where the receptor proteins act and where they should

in principle be measured). The second consideration is that a set of antibodies that are both highly specific to the individual mouse EphAs, and that at the same time bind to these proteins with the same affinity and signal-to-noise properties, are not yet available. In contrast, as is the case for the mRNAs of most transmembrane proteins, a substantial fraction of the EphA mRNAs are retained within RGC cell bodies in close association with the ER. Reber et al. (2004) therefore performed quantitative *in situ* hybridization to determine the relative expression levels of the *EphA4*, *A5*, and *A6* mRNAs in RGCs across the tn axis of the mouse retina. In doing so, these researchers assumed that measured differences in mRNA expression translate into linearly related differences in protein expression. Their measurements demonstrated that the aggregate mouse EphA ( $\Sigma$ EphA) retinal gradient is indeed well fit by an exponential plus a constant, i.e.,

$$C(x) = 0.26e^{0.023x} + 1.05,$$

where  $C_{v0}$  is 0.26,  $k$  is 0.023 and  $C_4$  is 1.05 (Reber et al. 2004). These investigators then used the same methods to measure the expression level of *EphA3* mRNA in the *EphA3*<sup>+</sup> (*Isl2*<sup>+</sup>) RGCs of both *Isl2-EphA3* heterozygous and homozygous knock-ins. These measurements demonstrated that the level of this mRNA is approximately constant across the tn axis of the knock-ins and that the heterozygote signal is ~50% of the homozygote signal (Reber et al. 2004). When the measured *EphA3* “spikes,” corresponding to the subset of RGCs that are *Isl2*<sup>+</sup>, were added to the wild-type  $\Sigma$ EphA curve, the quasi-oscillatory EphA gradients of the *Isl2-EphA3* heterozygotes and homozygotes were obtained (Figure 8).

**Molecular genetic tests of the relative signaling model.** Reber and colleagues used these measured EphA gradients to examine mapping collapse in the heterozygous knock-ins. These investigators proposed that col-

lapse occurs at the point at which the ratio of EphA signaling between an *EphA3*<sup>+</sup> RGC and an immediately adjacent *EphA3*<sup>-</sup> RGC—designated the  $R_{lrs}$ —becomes too low for the mapping system to discriminate. The measured gradients in the knock-ins allowed these investigators to assign this “discrimination limit” ratio the value of 1.36: This is the value of  $R_{lrs}$  at 76% of the retinal axis in the heterozygous knock-ins, the point at which mapping collapse occurs (Figure 8). In this formulation, two RGCs whose signaling difference is below this value are topographically indistinguishable. The  $R_{lrs}$  function, which describes how  $R_{lrs}$  varies across the tn axis, never reaches this value in the homozygous knock-ins; this is consistent with the fact that the retinocollicular map in these mice does not collapse (Figure 8, Reber et al. 2004).

This  $R_{lrs}$  function and the discrimination limit turned out to have remarkable predictive power with respect to mapping behavior in the *Isl2-EphA3* knock-ins. Reber and colleagues generated compound mutant mice that were heterozygous or homozygous for the *Isl2-EphA3* knock-in and at the same time heterozygous or homozygous for the knockout of the *EphA4* gene. Each of these compound mutants has a distinct  $R_{lrs}$  function that predicts if, and if so, where, mapping collapse occurs (Reber et al. 2004). The authors anatomically measured the retinocollicular maps in each genotype and demonstrated that each of the predictions made by the  $R_{lrs}$  functions was confirmed in the measured map of each genotype. In addition to defining a minimum  $R_{lrs}$  value (1.36) below which two RGCs are topographically identical, Reber and colleagues also presented evidence from their mapping analyses in the compound *Isl2-EphA3/EphA4* mutant genotypes that there is a maximum value for  $R_{lrs}$  at which two RGCs are maximally different (maximally separated) in terms of their topographic mapping to the SC. Perhaps not surprisingly, this value turns out to be 2.75—the ratio in EphA expression observed between the temporal and nasal poles of the wild-type mouse retina.

---

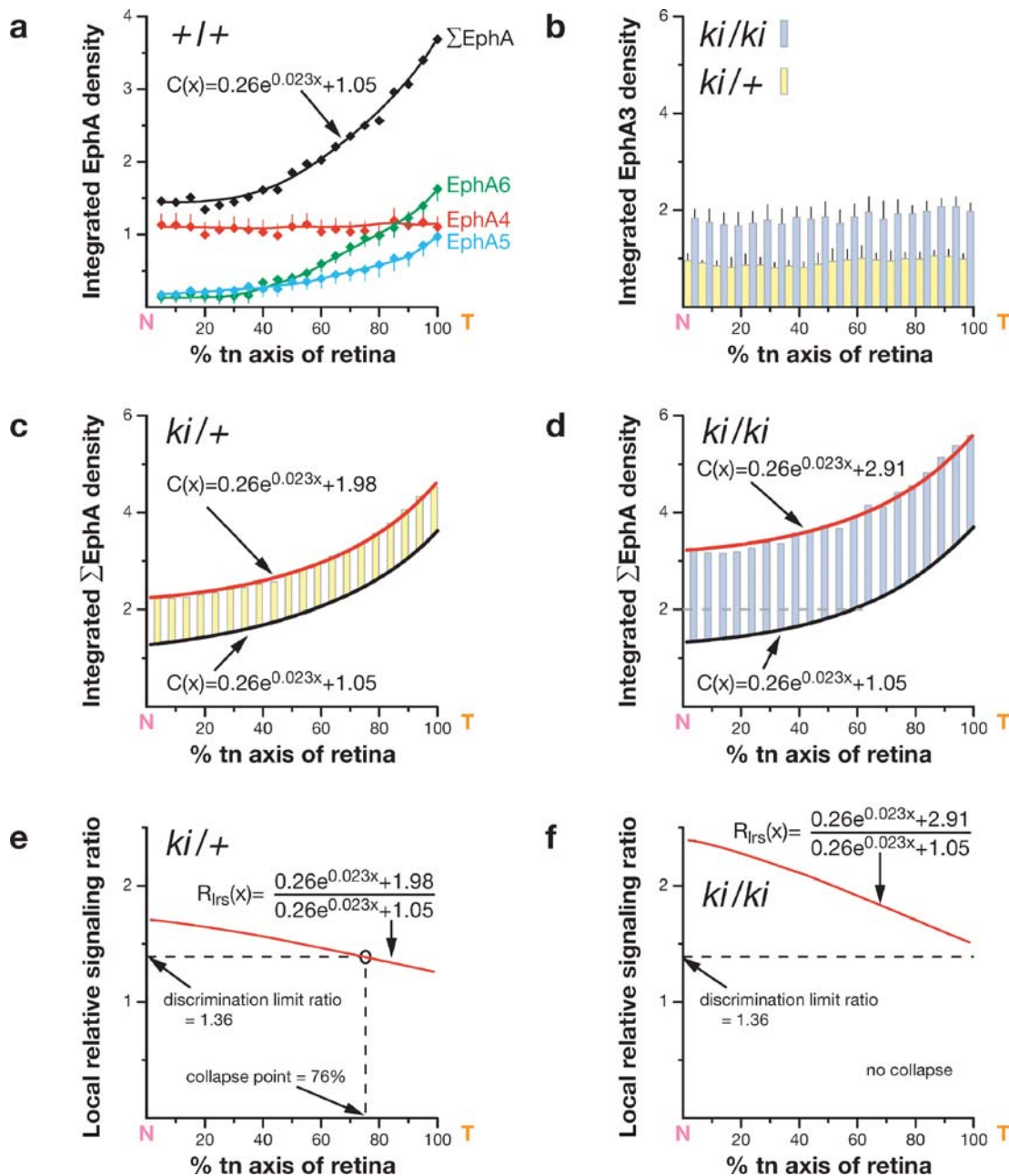
$R_{lrs}$ : local relative signaling ratio

---



The analysis of the compound mutants generated by Reber and colleagues—notably with respect to the rostral-caudal extent of TZ separation in the knock-ins—also addressed one possible role for ephrin-As in the retina. As mentioned above, these ephrin-As run in a

countergradient, from high nasal to low temporal, to EphA5 and EphA6 (Marcus et al. 1996, Hornberger et al. 1999). Retinal ephrin-As have been proposed to act locally in retinal organization or to be delivered, via RGC axons, to the SC, where they can participate





in map refinement (McLaughlin & O'Leary 1999, Yates et al. 2001). Another possibility is that these ligands sharpen the EphA functional gradient by inactivating nasally the EphA4 receptor (Connor et al. 1998, Hornberger et al. 1999, Menzel et al. 2001). Results from Reber and colleagues tend to argue against the latter possibility. If EphA4 function were fully graded—that is, if this receptor were completely inactivated in the nasal retina—then the removal of half or the entire EphA4 contribution to the  $\Sigma$ EphA gradient should have little or no effect on the projections of the nasal retinal axons. Alternatively, if EphA4 function were, like EphA4 expression, not graded in the retina, then removing some or all EphA4 should have very large effects on the projections of the nasal retinal axons. This latter phenomenon was in fact observed (Reber et al. 2004).

### Relative signaling and the wild-type map.

Reber and colleagues went on to propose a relative signaling explanation for the formation of the normal retinocollicular map. This explanation, which is again based on the hypoth-

esis that topographic mapping order along the tn axis is dependent on a ratiometric comparison of EphA-signaling intensity, represents a generalized extension of the local relative signaling phenomena of the knock-ins to the entire RGC ensemble of the normal eye (Reber et al. 2004). In the case of the smoothly and gradually increasing  $\Sigma$ EphA gradient of the wild-type retina, the local RS ratio carries almost no information. This ratio is only trivially different from 1.0 as adjacent RGCs along the wild-type axis have essentially the same level of  $\Sigma$ EphA. So how are local RS comparisons made in the context of the ensemble-wide competition that leads to formation of the wild-type retinocollicular map?

As noted above, map formation in most vertebrates takes place during a week-long period of competition between RGC axons for innervation targets in the SC (Simon et al. 1992, Yates et al. 2001, Hindges et al. 2002). If ratiometric comparisons of  $\Sigma$ EphA are used to set the rules by which RGCs compete for a limiting feature of the SC during this time, the dominant cell in the ensemble will be the

### Figure 8

Relative signaling in retinocollicular mapping. (a) Quantitation of the *EphA4*, *EphA5*, and *EphA6* mRNA gradients across the tn axis of the wild-type mouse retina, as described by Reber et al. (2004). Summing each of the measured values at each point yields  $\Sigma$ EphA, the aggregate level of *EphA* mRNA. As demanded by the relative signaling formulations, the  $\Sigma$ EphA gradient is described by the indicated equation: an exponential plus a constant. (b) Quantitation of the intermittent expression of *EphA3* mRNA in the *Isl2*<sup>+</sup> RGCs of *Isl2-EphA3* heterozygotes (ki/+, yellow bars) and homozygotes (ki/ki, light blue bars). (c) The  $\Sigma$ EphA gradient of *Isl2-EphA3* heterozygotes. The ki/+ *EphA3* "spikes" in b are superimposed onto the wild-type  $\Sigma$ EphA curve of a (bottom equation, curve). The red curve, which is described by the indicated equation, connects the tops of the spikes and corresponds to the  $\Sigma$ EphA gradient of the *EphA3*<sup>+</sup> RGCs. (d) The  $\Sigma$ EphA gradient of *Isl2-EphA3* homozygotes. The ki/ki *EphA3* "spikes" in b are superimposed onto the wild-type  $\Sigma$ EphA curve of a (bottom equation, curve). The red curve, which is described by the indicated equation, corresponds to the  $\Sigma$ EphA gradient of the *EphA3*<sup>+</sup> RGCs. (e) The local relative signaling ratio ( $R_{\text{IRS}}$ ) function of *Isl2-EphA3* heterozygotes. This function describes how  $R_{\text{IRS}}$ —the ratiometric difference in  $\Sigma$ EphA expression between an *EphA3*<sup>+</sup> RGC and an immediately adjacent *EphA3*<sup>-</sup> RGC—varies with position along the tn axis of the retina.  $R_{\text{IRS}}$  is described by dividing the right-hand sides of the upper and lower equations in c. The discrimination limit ratio (1.36) is the ratiometric difference limit below which two RGCs map to the same rostral-caudal collicular location and is defined by the collapse point of the *Isl2-EphA3* heterozygote map (Figure 7c). (f) The  $R_{\text{IRS}}$  function of *Isl2-EphA3* homozygotes, generated as for the heterozygotes in e. (The homozygote  $R_{\text{IRS}}$  function is described by dividing the right-hand sides of the upper and lower equations in d.) Modified from Reber et al. (2004), with permission from Nature (<http://www.nature.com>), copyright 2004 by Macmillan Publishers Ltd.

---

**R<sub>grs</sub>**: general relative signaling ratio

**BDNF**: brain-derived neurotrophic factor

---

neuron with the highest levels of  $\Sigma$ EphA signaling and the greatest sensitivity to the collicular ephrin-As, i.e., the RGC located at the temporal pole of the retina. (As also noted above, temporal RGCs are indeed most sensitive to chemorepulsion by ephrin-As.) In this milieu, all RGCs may compare themselves to all other RGCs by calculating a general signaling ratio relative to this same temporal reference.

Thirty years ago, Prestige & Wilshaw (1975) advanced, on purely theoretical grounds, a compelling case for a dominant polar reference cell of this form in so-called competition-by-exclusion models of retinotectal mapping. In the formulation of Reber et al. (2004), the highest  $R_{grs}$  will be the temporal/nasal  $\Sigma$ EphA ratio of RGCs at the nasal pole of the retina. Increasingly more temporal RGCs will have increasingly lower ratios, reaching 1.0 at the temporal pole. Most importantly, the model requires that the  $R_{grs}$  function—which describes the ratio between the temporal pole and RGCs all along the retinal axis—must yield, i.e., be identical to, the retinocollicular map of wild-type mice. Reber and colleagues demonstrated that this is indeed the case (**Figure 9**).

**EphA ratios and axon competition in the SC.** The ratiometric signaling parameters established by the  $\Sigma$ EphA gradient in the retina somehow must be transferred to competitive interactions between RGC axons that result in the topographically correct innervation of the axons' targets in the SC. Reber et al. (2004) speculated that competition of RGC axons for some limiting feature of the SC may itself be mediated by relative signaling and that a candidate for the limiting collicular feature is BDNF. This neurotrophin is expressed in the SC during the period of map formation and is a potent inducer of collateral branching by RGC axons. It is also a well-known stabilizer of nascent synaptic connections throughout the CNS (Alsina et al. 2001). RGC axons express TrkB, the receptor for BDNF (Suzuki et al. 1998).

Reber et al. (2004) suggest that relative signaling through the EphA receptor system might be translated into biased competition for BDNF through biased axon branching. As noted above, at the start of the axon competition events that mediate topographic mapping (around P0 in the mouse), nearly all primary axons occupy the full rostral-caudal extent of the SC. As competition ensues, RGC axons with low  $\Sigma$ EphA (i.e., nasal axons) are relatively insensitive to the inhibitory effects of collicular ephrin-As and therefore attempt to branch all along the collicular axis. In contrast, axons with high  $\Sigma$ EphA (i.e., temporal axons) extend many fewer branches and only in the most rostral regions of the axis. Reber and colleagues suggest that if the concentration of BDNF in the SC is limiting with respect to the number of RGC axons and their branches, then the difference in the extent of branch extension between nasal and temporal RGC axons is translated over time into a local difference in the intensity of BDNF/TrkB signaling at each location along the caudal-rostral axis of the SC. This occurs because the membrane density of TrkB receptors at any given point in a nasal axon is lower than in a temporal axon at the same position because the former axon has distributed its available TrkB protein over many more collateral branches that occupy more membrane area. According to this speculation, the local membrane density of TrkB receptors becomes progressively lower in progressively more caudal regions of the SC in exact proportion to the variation in the level of  $\Sigma$ EphA along the tn axis of the retina (Reber et al. 2004). An  $\Sigma$ EphA-directed biasing of local TrkB signaling of this form will occur even if all RGCs express the same level of TrkB per cell (Reber et al. 2004).

**Relative signaling in relation to earlier models.** The relative signaling model stands in contrast to earlier models of retinotectal mapping. Many of these were purely theoretical and, because the gradients of hypothesized signaling molecules were neither known nor measured, could not be tested

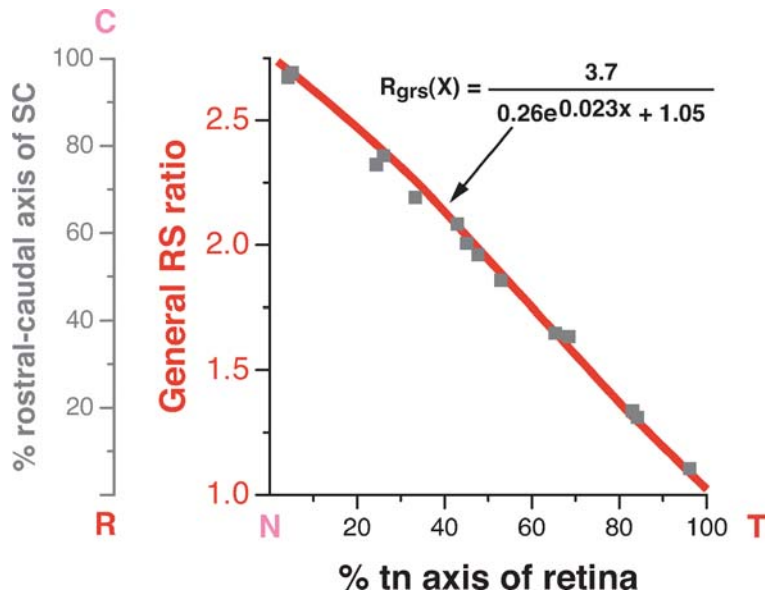


**Figure 9**

Relative signaling yields the wild-type mouse retinocollicular map. The indicated equation is the  $R_{grs}$  function for wild-type mice and is plotted as the red curve. The equation describes the ratio of  $\Sigma$ EphA at the temporal pole of the retina (3.7) divided by the term that describes the  $\Sigma$ EphA gradient along the tn axis of the retina.  $R_{grs}$  varies from a maximum of 2.75 (temporal pole/nasal pole) to a minimum of 1 (temporal pole/temporal pole). The gray data points are those of **Figure 7b** (plotted on the gray y axis), and correspond to the wild-type mouse retinocollicular map. Modified from Reber et al. (2004) with permission from Nature (<http://www.nature.com>), copyright 2004 by Macmillan Publishers Ltd.

experimentally. They generally invoked the presence of multiple gradients (Gierer 1983, 1987). In the absence of RGC axon competition in the SC, even a rostral-caudal chemorepellent gradient in the SC coupled to a tn receptor gradient in the retina requires additional gradients for topographic specificity and tight TZs. These additional gradients might include a chemoattractant gradient in the SC that parallels the ephrin-A chemorepellent gradient (O'Leary et al. 1999). The evidence for additional gradients at this point remains circumstantial, although a role for ephrin-A-mediated reverse signaling, which is compatible with the relative signaling formulations of Reber et al. (2004), is certainly plausible.

As noted above, simple mass-action models of mapping, in which topographic mapping is determined by a threshold ligand (L)-receptor (R) interaction that yields a sig-

naling complex RL (e.g., Nakamoto et al. 1996), have not been supported by the results of molecular genetic manipulations of Eph receptors and their ligands (Feldheim et al. 2000, Brown et al. 2000). Instead, the phenotypes of *ephrin-A2/-A5* double knock-outs and the *Isl2-EphA3* knock-ins are most straightforwardly explained by a scenario in which RGCs are forced to compete with one another for a limiting feature of the SC and in which the rules for this competition are set by ratiometric comparisons of EphA signaling intensity (Reber et al. 2004). The limiting collicular feature in theory might be space (innervation sites on postsynaptic cells) or a neurotrophic factor that stimulates branch formation and/or stabilizes synapses. Indeed, the behavior of wild-type axons in the *Isl2-EphA3* homozygous knock-ins—in which these axons are pushed to progressively more caudal locations in the SC as one moves to progressively

more temporal retinal locations (Brown et al. 2000)—is difficult to account for by any mechanism other than simple competition.

**The generality of relative signaling.** Relative signaling may apply to many instances in development in which competition between cells operates. In the nervous system, survival of nascent neurons based on access to neurotrophins (Van Ooyen & Willshaw 1999, Van Ooyen 2001), stabilization of synapses in the neocortex (Vicario-Abejon et al. 2002), and innervation of muscle targets by motor neurons through the elimination of ectopic synapses (Van Ooyen 2001) are all thought to depend upon competition. Each of these competitive events is dynamic and takes place over an extended period of time. They result in the establishment of innervation order, the numerical matching of input and output cells, or both. The demonstration that developing ensembles of competing RGCs perform comparisons on the basis of ratios rather than absolute differences—that is, that competing RGCs divide rather than subtract to establish order—suggests that ratiometric comparisons of signaling intensity may operate in these other instances as well.

### Computational Approaches

Few subjects in developmental neurobiology have been as extensively and repeatedly modeled as retinotectal mapping (Prestige & Willshaw 1975; Fraser & Hunt 1980; Gierer 1981; Whitelaw & Cowan 1981; Fraser & Perkel 1990; Goodhill 1998; Goodhill & Urbach 1999; Loschinger et al. 2000; Honda 2003, 2004; Reber et al. 2004; Yates et al. 2004). Beginning in the 1970s, many of these models were implemented in computer programs that dynamically simulated map development. Among the first of these was a simulation based on “systems matching”: the idea that RGC axons compete for limiting tectal space. In such models, retinal and tectal gradients of hypothetical labels were configured to run in the same direction. All retinal ax-

ons competed for the tectal site displaying the highest label but only the RGCs carrying the highest cognate label synapsed (Prestige & Willshaw 1975). Several groups proposed and implemented more-abstract systems matching models that contained a variety of additional biological constraints. These were typically based on reaching an optimal balance between opposing forces of competition and systems matching; this balance was achieved through the action of stable linear or exponential gradients (Fraser & Hunt 1980, Gierer 1981, Whitelaw & Cowan 1981, Fraser & Perkel 1990). A major concern of the models was whether they could mimic the results of both retinal/tectal ablation and rotation perturbations as well as those of developmental studies (Holt & Harris 1983, Holt 1984, Sakaguchi & Murphey 1985, Stuemmer 1988). Many researchers were, in fact, able to do this, but because they lacked any information as to the identity of the molecules that make up the gradients or their bioactivity, their expression level, or their graded distributions during development, these models remained theoretical exercises.

The identification of the Eph receptors and their ephrin ligands, the observation and quantitation of their graded distributions in the retina and tectum, and the discovery of their chemorepellent and chemoattractant activities have grounded the models in biological reality. Modifications of the mass-action model, including the mass-action/set-point rule model (Goodhill & Richards 1999), the imprinting-matching model (Loschinger et al. 2000), and the servomechanism-competition model (Honda 2003, 2004) have incorporated these known gradients and have included some biologically relevant constraints such as competition and colocalization of receptor and ligands. The latest of these efforts comes much closer to reproducing the mapping phenomena seen following molecular genetic manipulations, notably those evident in the *ephrin-A2/-A5* knockouts and the *Isl2-EphA3* knock-ins (Koulakov & Tsigankov 2004). The recent quantitation

of each of the constituent receptors of the EphA gradient in the mouse retina, together with the molecular genetic demonstration that EphA signaling differences may be interpreted ratiometrically (Reber et al. 2004), should allow for more powerful refinement of these computational models of mapping.

## CONCLUSIONS

The mouse mutant findings summarized above demonstrate that EphA signaling is essential to the mapping of the tn axis of the retina onto the rostral-caudal axis of the tectum and, similarly, that EphB signaling is required for the accurate mapping of the dorsal-ventral axis of the retina onto the lateral-medial axis of the tectum. They further show that these Eph signaling systems operate in the context of ensemble-wide neuronal competition. Analysis of the *Isl2-EphA3* knock-ins, both alone and in combination with *EphA4* knockouts, demonstrates that EphA signaling comparisons within the RGC ensemble are made—and retinotectal mapping is thereby ordered—on the basis of relative and not absolute differences in signaling

intensity. The relative signaling equations of Reber et al. (2004) demonstrate that ratiometric comparison of EphA signaling between the temporal pole RGC of the retina and all other RGCs along the tn axis yields the wild-type retinocollicular map.

Although each of these demonstrations represents significant advances, important questions remain: Do the orthogonally arrayed EphA and EphB signaling systems interact? How important is “reverse signaling” in either system? In what contexts might ephrin-As function as chemoattractants as well as chemorepellents? (See, for example, Hansen et al. 2004.) It is possible to address these questions using molecular genetics, but sophisticated approaches that go beyond “plain vanilla” knockouts will be required. Both Ephs and ephrins are expressed in both the retina and the tectum, can act as both chemoattractants and chemorepellents, and can serve as both receptors and ligands. These considerations argue for future conditional or inducible genetic manipulations that, as with the *Isl2-EphA3* knock-ins, are confined to a defined population of cells in either the retina or the tectum, but not both.

## LITERATURE CITED

- Alsina B, Vu T, Cohen-Cory S. 2001. Visualizing synapse formation in arborizing optic axons in vivo: dynamics and modulation by BDNF. *Nat. Neurosci.* 4:1093–101
- Arora HL, Sperry RW. 1962. Optic nerve regeneration after surgical cross-union of medial and lateral optic tracts. *Am. Zool.* 2:389
- Attardi DG, Sperry RW. 1963. Preferential selection of central pathways by regenerating optic fibers. *Exp. Neurol.* 7:46–64
- Attardi DG, Sperry RW. 1960. Central routes taken by regenerating optic fibers. *Physiologist* 3:12
- Birgbauer E, Cowan CA, Sretavan DW, Henkemeyer M. 2000. Kinase independent function of EphB receptors in retinal axon pathfinding to the optic disc from dorsal but not ventral retina. *Development* 127:1231–41
- Braisted JE, McLaughlin T, Wang HU, Friedman GC, Anderson DJ, et al. 1997. Graded and lamina-specific distributions of ligands of EphB receptor tyrosine kinases in the developing retinotectal system. *Dev. Biol.* 191:14–28
- Brambilla R, Schnapp A, Casagrande F, Labrador JP, Bergemann AD, et al. 1995. Membrane-bound LERK2 ligand can signal through three different Eph-related receptor tyrosine kinases. *EMBO J.* 14:3116–26



---

This paper provides strong evidence that topographic order is determined by relative rather than fixed EphA levels, and RGCs compete for a limiting feature of the SC during mapping.

---

This paper was among the first to demonstrate that EphA receptors and their ligands are graded in the retina and tectum in a manner consistent with the chemoaffinity hypothesis.

---

---

This paper describes the dramatic phenotypes apparent in mice doubly mutant for ephrin-A2 and ephrin-A5; this leads to a substantial degradation of topographic mapping along the retinal tn axis.

---

- Brennan C, Monschau B, Lindberg R, Guthrie B, Drescher U, et al. 1997. Two Eph receptor tyrosine kinase ligands control axon growth and may be involved in the creation of the retinotectal map in the zebrafish. *Development* 124:655–64
- Brown A, Yates PA, Burrola P, Ortuno D, Vaidya A, et al. 2000. Topographic mapping from the retina to the midbrain is controlled by relative but not absolute levels of EphA receptor signaling. *Cell* 102:77–88**
- Cheng HJ, Nakamoto M, Bergemann AD, Flanagan JG. 1995. Complementary gradients in expression and binding of ELF-1 and Mek4 in development of the topographic retinotectal projection map. *Cell* 82:371–81**
- Cohen YE, Knudsen EI. 1999. Maps versus clusters: different representations of auditory space in the midbrain and forebrain. *Trends Neurosci.* 22:128–35
- Connor RJ, Menzel P, Pasquale EB. 1998. Expression and tyrosine phosphorylation of Eph receptors suggest multiple mechanisms in patterning of the visual system. *Dev. Biol.* 193:21–35
- Cook JE. 1979. Interactions between optic fibres controlling the locations of their terminals in the goldfish optic tectum. *J. Embryol. Exp. Morphol.* 52:89–103
- Cox EC, Muller B, Bonhoeffer F. 1990. Axonal guidance in the chick visual system: posterior tectal membranes induce collapse of growth cones from the temporal retina. *Neuron* 4:31–37
- Debski EA, Cline HT. 2002. Activity-dependent mapping in the retinotectal projection. *Curr. Opin. Neurobiol.* 12:93–99
- Donoghue MJ, Lewis RM, Merlie JP, Sanes JR. 1996. The Eph kinase ligand AL-1 is expressed by rostral muscles and inhibits outgrowth from caudal neurons. *Mol. Cell. Neurosci.* 8:185–98
- Drescher U, Kremoser C, Handwerker C, Loschinger J, Noda M, et al. 1995. In vitro guidance of retinal ganglion cell axons by RAGS, a 25 kDa tectal protein related to ligands for Eph receptor tyrosine kinases. *Cell* 82:359–70
- Dutting D, Handwerker C, Drescher U. 1999. Topographic targeting and pathfinding errors of retinal axons following overexpression of ephrinA ligands on retinal ganglion cell axons. *Dev. Biol.* 216:297–311
- Echteler SM, Nofsinger YC. 2000. Development of ganglion cell topography in the postnatal cochlea. *J. Comp. Neurol.* 425:436–46
- Feldheim DA, Kim YI, Bergemann AD, Frisen J, Barbacid M, et al. 2000. Genetic analysis of ephrin-A2 and ephrin-A5 shows their requirement in multiple aspects of retinocollicular mapping. *Neuron* 25:563–74**
- Feldheim DA, Nakamoto M, Osterfield M, Gale NW, DeChiara TM, et al. 2004. Loss-of-function analysis of EphA receptors in retinotectal mapping. *J. Neurosci.* 24:2542–50
- Feldheim DA, Vanderhaeghen P, Hansen MJ, Frisen J, Lu Q, et al. 1998. Topographic guidance labels in a sensory projection to the forebrain. *Neuron* 21:1303–13
- Flanagan JG, Vanderhaeghen P. 1998. The ephrins and Eph receptors in neural development. *Annu. Rev. Neurosci.* 21:309–45
- Fraser SE, Hunt RK. 1980. Retinotectal specificity: models and experiments in search of a mapping function. *Annu. Rev. Neurosci.* 3:319–52
- Fraser SE, Perkel DH. 1990. Competitive and positional cues in the patterning of nerve connections. *J. Neurobiol.* 21:51–72
- Friauf E, Lohmann C. 1999. Development of auditory brainstem circuitry. Activity-dependent and activity-independent processes. *Cell Tissue Res.* 297:187–95



- Frisen J, Yates PA, McLaughlin T, Friedman GC, O'Leary DD, et al. 1998. Ephrin-A5 (AL-1/RAGS) is essential for proper retinal axon guidance and topographic mapping in the mammalian visual system. *Neuron* 20:235–43
- Gale NW, Holland SJ, Valenzuela DM, Flenniken A, Pan L, et al. 1996. Eph receptors and ligands comprise two major specificity subclasses and are reciprocally compartmentalized during embryogenesis. *Neuron* 17:9–19
- Gaze RM, Fawcett JW. 1983. Pathways of *Xenopus* optic fibres regenerating from normal and compound eyes under various conditions. *J. Embryol. Exp. Morphol.* 73:17–38
- Gierer A. 1981. Generation of biological patterns and form: some physical, mathematical, and logical aspects. *Prog. Biophys. Mol. Biol.* 37:1–47
- Gierer A. 1983. Model for the retino-tectal projection. *Proc. R. Soc. London Ser. B* 218:77–93
- Gierer A. 1987. Directional cues for growing axons forming the retinotectal projection. *Development* 101:479–89
- Godement P, Bonhoeffer F. 1989. Cross-species recognition of tectal cues by retinal fibers in vitro. *Development* 106:313–20
- Goodhill GJ. 1998. Mathematical guidance for axons. *Trends Neurosci.* 21:226–31
- Goodhill GJ, Richards LJ. 1999. Retinotectal maps: molecules, models and misplaced data. *Trends Neurosci.* 22:529–34
- Goodhill GJ, Urbach JS. 1999. Theoretical analysis of gradient detection by growth cones. *J. Neurobiol.* 41:230–41
- Hansen MJ, Dallal GE, Flanagan JG. 2004. Retinal axon response to ephrin-As shows a graded, concentration-dependent transition from growth promotion to inhibition. *Neuron* 42:717–30
- Henkemeyer M, Orioli D, Henderson JT, Saxton TM, Roder J, et al. 1996. Nuk controls pathfinding of commissural axons in the mammalian central nervous system. *Cell* 86:35–46
- Hindges R, McLaughlin T, Genoud N, Henkemeyer M, O'Leary DD. 2002. EphB forward signaling controls directional branch extension and arborization required for dorsal-ventral retinotopic mapping. *Neuron* 35:475–87**
- Holash JA, Pasquale EB. 1995. Polarized expression of the receptor protein tyrosine kinase *Cek5* in the developing avian visual system. *Dev. Biol.* 172:683–93
- Holt CE, Harris WA. 1983. Order in the initial retinotectal map in *Xenopus*: a new technique for labelling growing nerve fibres. *Nature* 301:150–52
- Holt CE. 1984. Does timing of axon outgrowth influence initial retinotectal topography in *Xenopus*? *J. Neurosci.* 4:1130–52
- Holt CE, Harris WA. 1993. Position, guidance, and mapping in the developing visual system. *J. Neurobiol.* 24:1400–22
- Holt CE, Harris WA. 1998. Target selection: invasion, mapping and cell choice. *Curr. Opin. Neurobiol.* 8:98–105
- Honda H. 2003. Competition between retinal ganglion axons for targets under the servomechanism model explains abnormal retinocollicular projection of Eph receptor-overexpressing or ephrin-lacking mice. *J. Neurosci.* 23:10368–77
- Honda H. 2004. Competitive interactions between retinal ganglion axons for tectal targets explain plasticity of retinotectal projection in the servomechanism model of retinotectal mapping. *Dev. Growth Differ.* 46:425–37
- Hornberger MR, Dutting D, Ciossek T, Yamada T, Handwerker C, et al. 1999. Modulation of EphA receptor function by coexpressed ephrinA ligands on retinal ganglion cell axons. *Neuron* 22:731–42

---

This paper, analyzing mice doubly mutant for EphB2 and EphB3, indicates that the EphB signaling system is required for accurate mapping along the medial-lateral axis of the tectum, and that the system primarily acts to direct the medial growth up an ephrin-B gradient.

---

- Huh GS, Boulanger LM, Du H, Riqueline PA, Brotz TM, et al. 2000. Functional requirement for class I MHC in CNS development and plasticity. *Science* 290:2155–59
- Kaas JH. 1997. Topographic maps are fundamental to sensory processing. *Brain Res. Bull.* 44:107–12
- Kanaseki T, Sprague JM. 1974. Anatomical organization of pretectal nuclei and tectal laminae in the cat. *J. Comp. Neurol.* 158:319–37
- King AJ, Palmer AR. 1983. Cells responsive to free-field auditory stimuli in guinea-pig superior colliculus: distribution and response properties. *J. Physiol.* 342:361–81
- Knoll B, Isenmann S, Kilic E, Walkenhorst J, Engel S, et al. 2001. Graded expression patterns of ephrin-As in the superior colliculus after lesion of the adult mouse optic nerve. *Mech. Dev.* 106:119–27
- Knudsen EI. 1982. Auditory and visual maps of space in the optic tectum of the owl. *J. Neurosci.* 2:1177–94
- Koulakov AA, Tsiganov DN. 2004. A stochastic model for retinocollicular map development. *BMC Neurosci.* 5:30–47
- Kullander K, Klein R. 2002. Mechanisms and functions of Eph and ephrin signalling. *Nat. Rev. Mol. Cell Biol.* 3:475–86
- Loschinger J, Weth F, Bonhoeffer F. 2000. Reading of concentration gradients by axonal growth cones. *Philos. Trans. R. Soc. London Ser. B* 355:971–82
- Mann F, Ray S, Harris W, Holt C. 2002. Topographic mapping in dorsoventral axis of the Xenopus retinotectal system depends on signaling through ephrin-B ligands. *Neuron* 35:461–73
- Marcus RC, Gale NW, Morrison ME, Mason CA, Yancopoulos GD. 1996. Eph family receptors and their ligands distribute in opposing gradients in the developing mouse retina. *Dev. Biol.* 180:786–89
- Marin O, Blanco MJ, Nieto MA. 2001. Differential expression of Eph receptors and ephrins correlates with the formation of topographic projections in primary and secondary visual circuits of the embryonic chick forebrain. *Dev. Biol.* 234:289–303
- McLaughlin T, Hindges R, Yates PA, O’Leary DD. 2003. Bifunctional action of ephrin-B1 as a repellent and attractant to control bidirectional branch extension in dorsal-ventral retinotopic mapping. *Development* 130:2407–18
- McLaughlin T, O’Leary DD. 1999. Functional consequences of coincident expression of EphA receptors and ephrin-A ligands. *Neuron* 22:636–39
- Menzel P, Valencia F, Godement P, Dodelet VC, Pasquale EB. 2001. Ephrin-A6, a new ligand for EphA receptors in the developing visual system. *Dev. Biol.* 230:74–88
- Meyer RL. 1982. Ordering of retinotectal connections: a multivariate operational analysis. *Curr. Top. Dev. Biol.* 17:101–45
- Monschau B, Kremoser C, Ohta K, Tanaka H, Kaneko T, et al. 1997. Shared and distinct functions of RAGS and ELF-1 in guiding retinal axons. *EMBO J.* 17:1258–67
- Murai K, Pasquale EB. 2003. ‘Eph’ective signaling: forward, reverse and crosstalk. *J. Cell Sci.* 116:2823–32
- Nakamoto M, Cheng HJ, Friedman GC, McLaughlin T, Hansen MJ, et al. 1996. Topographically specific effects of ELF-1 on retinal axon guidance in vitro and retinal axon mapping in vivo. *Cell* 86:755–66
- Nakamura H, O’Leary DD. 1989. Inaccuracies in initial growth and arborization of chick retinotectal axons followed by course corrections and axon remodeling to develop topographic order. *J. Neurosci.* 9:3776–95
- O’Leary DD, Fawcett JW, Cowan WM. 1986. Topographic targeting errors in the retinocollicular projection and their elimination by selective ganglion cell death. *J. Neurosci.* 6:3692–705

- O'Leary DD, Yates PA, McLaughlin T. 1999. Molecular development of sensory maps: representing sights and smells in the brain. *Cell* 96:255–69
- Park S, Frisen J, Barbacid M. 1997. Aberrant axonal projections in mice lacking EphA8 (Eek) tyrosine protein kinase receptors. *EMBO J.* 16:3106–14
- Penfield W, Rasmussen T. 1950. *The Cerebral Cortex of Man. A Clinical Study of Localization of Function.* New York: Macmillan
- Prestige MC, Willshaw DJ. 1975. On a role for competition in the formation of patterned neural connexions. *Proc. R. Soc. London Ser. B* 190:77–98
- Reber M, Burrola P, Lemke G. 2004. A relative signaling model for the formation of a topographic neural map. *Nature* 431:847–53**
- Rodieck RW. 1979. Visual pathways. *Annu. Rev. Neurosci.* 2:193–225
- Rogers JH, Ciossek T, Ullrich A, West E, Hoare M, et al. 1999. Distribution of the receptor EphA7 and its ligands in development of the mouse nervous system. *Brain Res. Mol. Brain Res.* 74:225–30
- Roskies AL, O'Leary DD. 1994. Control of topographic retinal axon branching by inhibitory membrane-bound molecules. *Science* 265:799–803
- Rubel EW, Cramer KS. 2002. Choosing axonal real estate: location, location, location. *J. Comp. Neurol.* 448:1–5
- Rubel EW, Fritzsche B. 2002. Auditory system development: primary auditory neurons and their targets. *Annu. Rev. Neurosci.* 25:51–101
- Sachs GM, Jacobson M, Caviness VS Jr. 1986. Postnatal changes in arborization patterns of murine retinocollicular axons. *J. Comp. Neurol.* 246:395–408
- Sakaguchi DS, Murphey RK. 1985. Map formation in the developing *Xenopus* retinotectal system: an examination of ganglion cell terminal arborizations. *J. Neurosci.* 5:3228–45
- Sakurai T, Wong E, Drescher U, Tanaka H, Jay DG. 2002. Ephrin-A5 restricts topographically specific arborization in the chick retinotectal projection in vivo. *Proc. Natl. Acad. Sci. USA* 99:10795–800
- Schmidt JT, Ciceron CM, Easter SS. 1978. Expansion of the half retina projection to the tectum in goldfish: an electrophysiological and anatomical study. *J. Comp. Neurol.* 177:257–78
- Sharma SC. 1972. Reformation of retinotectal projections after various tectal ablations in adult goldfish. *Exp. Neurol.* 34:171–82
- Simon DK, O'Leary DD. 1992a. Responses of retinal axons in vivo and in vitro to position-encoding molecules in the embryonic superior colliculus. *Neuron* 9:977–89
- Simon DK, O'Leary DD. 1992b. Development of topographic order in the mammalian retinocollicular projection. *J. Neurosci.* 12:1212–32
- Simon DK, O'Leary DD. 1992c. Influence of position along the medial-lateral axis of the superior colliculus on the topographic targeting and survival of retinal axons. *Brain Res. Dev. Brain Res.* 69:167–72
- Sperry RW. 1943. Effect of 180 degree rotation of the retinal field on visuomotor coordination. *J. Exp. Zool.* 92:263–79
- Sperry RW. 1944. Optic nerve regeneration with return of vision in anurans. *J. Neurophysiol.* 7:57–69
- Sperry RW. 1963. Chemoaffinity in the orderly growth of nerve fiber patterns and connections. *Proc. Natl. Acad. Sci. USA* 50:703–10**
- Stahl B, Muller B, von Boxberg Y, Cox EC, Bonhoeffer F. 1990. Biochemical characterization of a putative axonal guidance molecule of the chick visual system. *Neuron* 5:735–43
- Stuermer CA. 1988. Retinotopic organization of the developing retinotectal projection in the zebrafish embryo. *J. Neurosci.* 8:4513–30

---

This paper presents a quantitative analysis of the Isl2-EphA3 knock-ins, both alone and in combination with EphA4 knockouts. It provides the first comprehensive quantitative formulation of competitive neighbor interactions in retinotectal mapping.

---



---

This classic paper advances Roger Sperry's ideas with respect to chemoaffinity.

---

- Taylor JS, Gaze RM. 1985. The effects of the fibre environment on the paths taken by regenerating optic nerve fibres in *Xenopus*. *J. Embryol. Exp. Morphol.* 89:383–401
- van Ooyen A. 2001. Competition in the development of nerve connections: a review of models. *Network* 12:R1–47
- van Ooyen A, Willshaw DJ. 1999. Competition for neurotrophic factor in the development of nerve connections. *Proc. R. Soc. London Ser. B* 266:883–92
- Vicario-Abejon C, Owens D, McKay R, Segal M. 2002. Role of neurotrophins in central synapse formation and stabilization. *Nat. Rev. Neurosci.* 3:965–74
- Walter J, Henke-Fahle S, Bonhoeffer F. 1987a. Avoidance of posterior tectal membranes by temporal retinal axons. *Development* 101:909–13
- Walter J, Kern-Veits B, Huf J, Stolze B, Bonhoeffer F. 1987b. Recognition of position-specific properties of tectal cell membranes by retinal axons in vitro. *Development* 101:685–96
- Whitelaw VA, Cowan JD. 1981. Specificity and plasticity of retinotectal connections: a computational model. *J. Neurosci.* 1:1369–87
- Winslow JW, Moran P, Valverde J, Shih A, Yuan JQ, et al. 1995. Cloning of AL-1, a ligand for an Eph-related tyrosine kinase receptor involved in axon bundle formation. *Neuron* 14:973–81
- Yates PA, Holub AD, McLaughlin T, Sejnowski TJ, O’Leary DD. 2004. Computational modeling of retinotopic map development to define contributions of EphA-ephrinA gradients, axon-axon interactions, and patterned activity. *J. Neurobiol.* 59:95–113
- Yates PA, Roskies AL, McLaughlin T, O’Leary DD. 2001. Topographic-specific axon branching controlled by ephrin-As is the critical event in retinotectal map development. *J. Neurosci.* 21:8548–63
- Yoon M. 1976. Progress of topographic regulation of the visual projection in the halved optic tectum of adult goldfish. *J. Physiol.* 257:621–43
- Zhang JH, Cerretti DP, Yu T, Flanagan JG, Zhou R. 1996. Detection of ligands in regions anatomically connected to neurons expressing the Eph receptor Bsk: potential roles in neuron-target interaction. *J. Neurosci.* 16:7182–92



# Contents

Frontispiece <i>David D. Sabatini</i> .....	xiv
In AwE of Subcellular Complexity: 50 Years of Trespassing Boundaries Within the Cell <i>David D. Sabatini</i> .....	1
Mechanisms of Apoptosis Through Structural Biology <i>Nieng Yan and Yigong Shi</i> .....	35
Regulation of Protein Activities by Phosphoinositide Phosphates <i>Verena Niggli</i> .....	57
Principles of Lysosomal Membrane Digestion: Stimulation of Sphingolipid Degradation by Sphingolipid Activator Proteins and Anionic Lysosomal Lipids <i>Thomas Kolter and Konrad Sandhoff</i> .....	81
Cajal Bodies: A Long History of Discovery <i>Mario Cioce and Angus I. Lamond</i> .....	105
Assembly of Variant Histones into Chromatin <i>Steven Henikoff and Kami Ahmad</i> .....	133
Planar Cell Polarization: An Emerging Model Points in the Right Direction <i>Thomas J. Klein and Marek Mlodzik</i> .....	155
Molecular Mechanisms of Steroid Hormone Signaling in Plants <i>Grégory Vert, Jennifer L. Nembhauser, Niko Geldner, Fangxin Hong, and Joanne Chory</i> .....	177
Anisotropic Expansion of the Plant Cell Wall <i>Tobias I. Baskin</i> .....	203
RNA Transport and Local Control of Translation <i>Stefan Kindler, Huidong Wang, Dietmar Richter, and Henri Tiedge</i> .....	223

Rho GTPases: Biochemistry and Biology <i>Aron B. Jaffe and Alan Hall</i> .....	247
Spatial Control of Cell Expansion by the Plant Cytoskeleton <i>Laurie G. Smith and David G. Oppenheimer</i> .....	271
RNA Silencing Systems and Their Relevance to Plant Development <i>Frederick Meins, Jr., Azeddine Si-Ammour, and Todd Blevins</i> .....	297
Quorum Sensing: Cell-to-Cell Communication in Bacteria <i>Christopher M. Waters and Bonnie L. Bassler</i> .....	319
Pushing the Envelope: Structure, Function, and Dynamics of the Nuclear Periphery <i>Martin W. Hetzer, Tobias C. Walther, and Iain W. Mattaj</i> .....	347
Integrin Structure, Allostery, and Bidirectional Signaling <i>M.A. Arnaout, B. Mahalingam, and J.-P. Xiong</i> .....	381
Centrosomes in Cellular Regulation <i>Stephen Doxsey, Dannel McCollum, and William Theurkauf</i> .....	411
Endoplasmic Reticulum–Associated Degradation <i>Karin Römisch</i> .....	435
The Lymphatic Vasculature: Recent Progress and Paradigms <i>Guillermo Oliver and Kari Alitalo</i> .....	457
Regulation of Root Apical Meristem Development <i>Keni Jiang and Lewis J. Feldman</i> .....	485
Phagocytosis: At the Crossroads of Innate and Adaptive Immunity <i>Isabelle Futras and Michel Desjardins</i> .....	511
Protein Translocation by the Sec61/SecY Channel <i>Andrew R. Osborne, Tom A. Rapoport, and Bert van den Berg</i> .....	529
Retinotectal Mapping: New Insights from Molecular Genetics <i>Greg Lemke and Michael Reber</i> .....	551
In Vivo Imaging of Lymphocyte Trafficking <i>Cornelia Halin, J. Rodrigo Mora, Cenk Sumen, and Ulrich H. von Andrian</i> .....	581
Stem Cell Niche: Structure and Function <i>Linbeng Li and Ting Xie</i> .....	605
Docosahexaenoic Acid, Fatty Acid–Interacting Proteins, and Neuronal Function: Breastmilk and Fish Are Good for You <i>Joseph R. Marszalek and Harvey F. Lodish</i> .....	633
Specificity and Versatility in TGF- $\beta$ Signaling Through Smads <i>Xin-Hua Feng and Rik Derynck</i> .....	659



The Great Escape: When Cancer Cells Hijack the Genes for Chemotaxis and Motility <i>John Condeelis, Robert H. Singer, and Jeffrey E. Segall</i> .....	695
---	-----

## INDEXES

Subject Index .....	719
Cumulative Index of Contributing Authors, Volumes 17–21 .....	759
Cumulative Index of Chapter Titles, Volumes 17–21 .....	762

## ERRATA

An online log of corrections to *Annual Review of Cell and Developmental Biology* chapters may be found at <http://cellbio.annualreviews.org/errata.shtml>